RESEARCH REPORT SERIES

Surface waves and their effects on circulation

Final Report GABRP Project 1.2

David Griffin, Mark Hemer, Mike Herzfeld, Charles James and John Luick

GABRP Research Report Series Number 21

August 2017

DISCLAIMER

COPYRIGHT

THIS PUBLICATION MAY BE CITED AS:

Griffin, D., Hemer, M., Hertzfeld, M., James, C. and Luick, J. (2017). Surface waves and their effects on circulation. Final Report GABRP Project 1.2. Great Australian Bight Research Program, GABRP Research Report Series Number 21, 37pp.

CONTACT

Dr David Griffin
CSIRO
e: David.Griffin@csiro.au

FOR FURTHER INFORMATION

www.misa.net.au/GAB

GREAT AUSTRALIAN BIGHT RESEARCH PROGRAM

The Great Australian Bight Research Program is a collaboration between BP, CSIRO, the South Australian Research and Development Institute (SARDI, the University of Adelaide, and Flinders University. The Program aims to provide a whole-of-system understanding of the environmental, economic and social values of the region; providing an information source for all to use.

CONTENTS

LIST OF FIGURES

1. EXECUTIVE SUMMARY

We used two ocean modelling systems to evaluate the impact on ocean circulation of including ocean surface wave information in conjunction with wind information, rather than using wind information alone.

There is no doubt waves play a crucial role in the exchange of momentum and turbulence between the ocean and the atmosphere. What is unclear is whether it is becoming worthwhile to model these processes explicitly, rather than continuing to represent them with traditional approximations.

Nor is there doubt waves are responsible for Stokes Drift. Wave orbital motions are not closed ellipses, so water near the surface of the ocean moves a small fraction of the orbital distance after each wave goes past. What is unclear is whether, when you take the rotation of the Earth into account, and try to represent the effects of Stokes Drift in a hydrodynamic model, the net effect on surface drift is significantly different, and detectably more correct.

We found that including wave information in the modelling did not demonstrably improve our ability to simulate the thermal structure of the ocean, or transient ocean surface currents. The only quantity which was clearly altered by taking waves explicitly into account was the long-term mean surface drift. But here, our two models disagreed. In one (SHOC-wave), the classical Stokes Drift was completely cancelled out by the hydrodynamical response to the Stokes-Coriolis forcing. In the other (the COAWST branch of the ROMS model), an additional ~5cm/s shorewards drift eventuated. This velocity is high enough to take buoyant surface matter from the edge of the shelf to the shore within a month - significantly faster than if the effect of waves is ignored.

We did not resolve which of the two models is more correct. The drifter observations suggest SHOC's estimate of the surface drift was not improved by taking Stokes Drift into account at all, but this is in conflict with several other studies, and theoretical considerations. Future development of SHOC-wave should focus on diagnosing the apparently excessively-large near-surface amplitude of the 'anti-Stokes' response. A welcome improvement to COAWST would be to move the calculation of Stokes velocities from within ROMS to within SWAN, where the full directional wave spectrum can be integrated. This will make a fairly large change to the direction of the Stokes Drift, thereby significantly altering estimates of how quickly buoyant matter might be transported from the outer shelf to the coast.

2. INTRODUCTION

2.1 Overview

The Great Australian Bight (GAB) is well known to mariners for its strong winds and large waves, which frequently exceed 5m in the deep ocean (Figure 2.1.1, and Hemer et al. 2017). The ocean currents, in contrast, are rather weak compared with the neighbouring temperate regions of Australia (Figure 2.1.2). More precisely, high current speeds associated with eddies and boundary currents are what are 'missing' in the GAB. This means the relative importance of locally wind-driven currents is higher in the GAB than elsewhere. To obtain an accurate picture of the circulation of the GAB (the purpose of Theme 1), we therefore decided it was prudent to pay particular attention to the ways strong winds influence the circulation. We therefore conceived a sub-project (this one) to focus specifically on that.

Winds influence the ocean in many ways that we will not try to summarise here. Suffice it to say, however, that most numerical models of the ocean circulation include a wind forcing term that takes no explicit account for waves. By this we mean that the waves are only accounted for implicitly, in

some averaged or parameterized sense. The purpose of this sub-project of the Oceanography Theme was to implement and evaluate some of the latest refinements (see Appendix 5: Review of Wave-Ocean coupling) of how wind, wave and circulation models are coupled to each other, focusing on the intermediary role waves take in this coupling.

The two main 'approximations' we wanted to relax were

- coupling between Stokes Drift and circulation is zero
- turbulence depends on winds only, not waves.

Stokes Drift is the net (wave-averaged) motion that results from the passage of waves through a body of otherwise stationary water. It is a Lagrangian drift velocity that depends only on the properties of the waves. To a first approximation, the total surface drift can be estimated by simply adding the Stokes drift to the output of an ocean model. As discussed by Polton (2005), Ardhuin *et al.* (2009), Uchiyama (2010), Röhrs (2012) (for example), however, there are feedbacks and interactions with the Coriolis force that should also be taken into account, because they lead to a compensating Eulerian flow in the hydrodynamic model. This 'anti-Stokes' response has comparable depth-averaged transport, with weaker velocities distributed deeper into the water column.

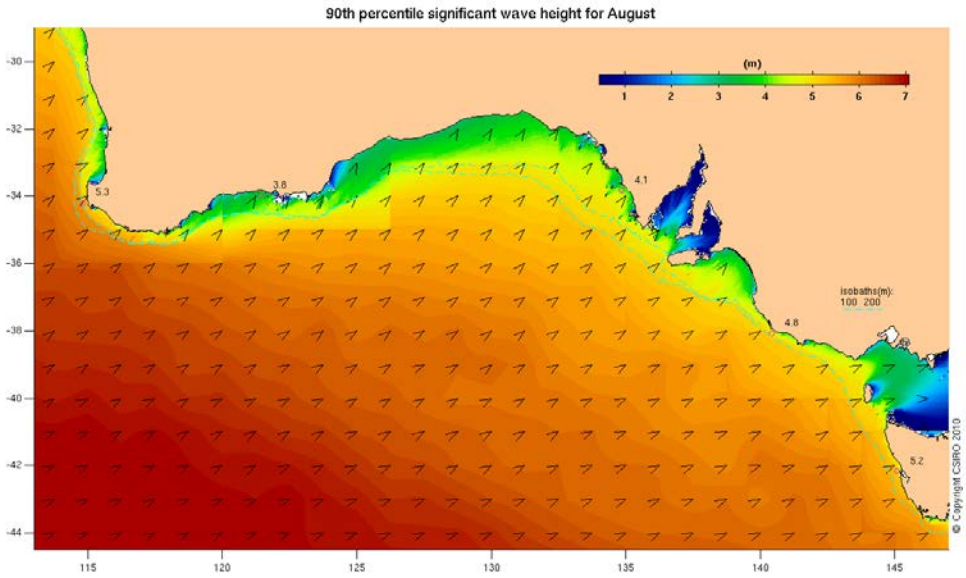

Figure 2.1.1 Significant wave height for August – 90th percentile. Arrow heads indicate the direction. Source: Hemer and Griffin (2010). [online: other months and percentiles]

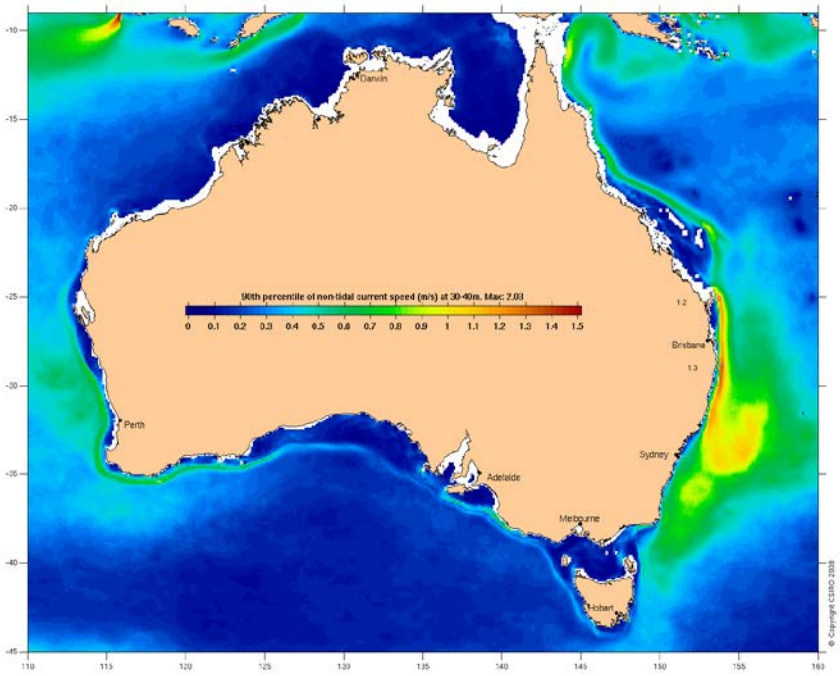

Figure 2.1.2 Non-tidal (daily-averaged) current speed – 90th percentile at 30-40m depth. Source: Griffin and Hemer (2008)

2.2 Objectives

The objectives were:

1. To estimate the effect of surface gravity waves (both swell and wind-waves) on
    a. surface and sub-surface transport of biota, nutrients and pollutants
    b. air-sea exchange of heat, freshwater (evaporation) and momentum
    c. turbulence throughout the water column
    d. bottom stress
2. To represent the time-dependent effects (as above) of surface gravity waves in numerical ocean circulation models.
3. To validate the improved performance of the circulation models as measured using various independent data.

Good progress was made towards all these objectives, as described below.

3. METHODS

This project is effectively a sub-project of Middleton et al. (2017). To avoid duplication, we will not reproduce the descriptions of the two modelling systems used by the GABRP Theme 1 participants, and will instead focus on the wave-specific numerical experiments that were conducted.

3.1 SHOC-Wave

A new version of SHOC (SHOC-Wave) was developed by CSIRO and implemented in the GAB as part of this project specifically to explicitly (rather than implicitly) account for many of the effects of waves on circulation. The converse - effect of circulation on waves - was not explored. This is therefore a one-way coupled configuration, in which a wave model is first run (forced by an atmospheric model), then the circulation model is run using the outputs of both the wave and atmosphere models as inputs.

Wave fields were taken from the CAWCR wave hindcast (Durrant et al. 2014, 2015) – a global implementation of WaveWatchIII (v4.08), with nested high resolution (4') around the Australian coast, providing good representation of wave characteristics in the region (Hemer et al., 2017). The simulated wave spectrum was represented using 29 frequency bins logarithmically spaced between 0.038 Hz and 0.5 Hz, with 24 directions with a constant 15 degree directional resolution. The wave model was forced with hourly surface winds and sea-ice concentrations taken from the NOAA Climate Forecast System Reanalysis, which has a spatial resolution of 0.4 degrees. The CAWCR hindcast archives over 30 integrated parameters of interest to the study, including standard wave variables (significant wave height, mean and peak wave period and directions), but also information on the atmosphere to wave, and wave to ocean components of the surface flux, and total integrated surface Stokes velocities. Importantly, the surface Stokes velocities are calculated within the wave model, using the full directional wave spectrum, as discussed below.

The parameterisations of wave-dependent processes implemented into SHOC were:

- Stokes-Coriolis and vortex force terms in the momentum equations (Moon, 2005)
- 2-D Radiation stress terms
- wave-dependent surface mixing, with several alternative mixing parameterisations including the BV method (Qiao et al., 2010), the wave orbital method (Ghantous and Babanin, 2014), the shallow water method of Jones and Monismith (2008), and a parameterization of Langmuir mixing derived by Harcourt (2012). These were implemented independently to ensure no double counting.
- adjustment of the surface stress to account for loss to wave generation, and return from wave decay.

The following wave fields were passed to the hydrodynamic model:

- surface Stokes velocity
- Stokes e-folding depth based on the peak wave period
- significant wave height and direction
- radiation stress components
- wave-supported wind-stress vector
- wave to ocean stress vector

3.2 SWAN-ROMS (COAWST)

The COAWST branch of the open-source ROMS model allows for two-way coupling of the hydrodynamic (circulation) model with the SWAN waves model. For brevity we will refer here to the coupled (SWAN-ROMS) model as COAWST and to the uncoupled hydrodynamic model as ROMS. SARDI configured both for the GAB domain.

COAWST couples the SWAN wave model (v40.91A) to the ROMS hydrodynamic model, and has improved simulation of wave-current interactions through the vortex-force method of computing Stokes currents (Uchiyama et al., 2010, Warner et al 2010, Kumar et al. 2012). The model was run for the 2 years from Dec 28 2010 to Dec 28 2012. The grid used was the SAM grid from Middleton et al. (2017) and the ROMS hydrodynamic model was run with the same forcing and setup (i.e. BRAN2015 boundary conditions and ECMWF atmospheric forcing).

The SWAN model was forced with 6 hourly 10m ECMWF winds from the ERA-Interim reanalysis. On the southern and western open boundaries, hourly integrated wave parameters (significant wave height, mean wave direction, mean wave period and directional spreading) from the CAWCR wave hindcast were used to define an assumed JONSWAP shaped spectrum with the default gamma (3.3). The simulated model wave spectrum was represented using 32 discrete frequencies equivalent to wave periods between 1 and 33.3 sec, and 24 directional bins (i.e., a directional resolution of 15 degrees).

The models exchanged the following 2D fields at half hour intervals:

SWAN to ROMS

- significant wave height and direction
- average wave length
- surface wave relative peak period
- bottom wave period
- wave energy dissipation
- percent wave breaking
- wave bottom orbital velocity

ROMS to SWAN

- bathymetry (static in this implementation)
- free surface elevation
- vertically integrated velocity
- bottom roughness

In addition to the ROMS settings used in the Middleton et al. (2017) model runs – the following coupling-specific features were activated during the simulation:

- wave-enhanced surface roughness
- wave-enhanced turbulent kinetic energy dissipation and vertical mixing
- vortex force wave-current interactions
- enhanced wave energy dissipation

3.3 Validation data

The IMOS HF radars are one of the key data sources for potentially validating the difference between models that do and don't take Stokes Drift into account. These measure the near-surface current velocity by measuring the Doppler shift of the radar signal returned by Bragg scattering from a narrow spectral band of the surface wave spectrum. The Doppler shift is due to the surface waves being advected by the surface current. The wavelength of the waves that do the scattering, and therefore the vertical decay scale of the wave orbital motions, is determined by the operating frequency of the radar, so this affects the effective sensing depth of the radar. The Bonney Coast CODAR senses the top ~8m while the South Australian Gulfs WERA array (Figure 3.3.1) senses the top ~5m. These depth intervals are larger than ideal for the purpose of validating estimates of the 'surface' drift (depth≈1m), but they are valuable for validating the model's estimates of the near-surface (0-5m) drift. For comparing with these data, we therefore do appropriate vertical averaging of the modelled velocity field.

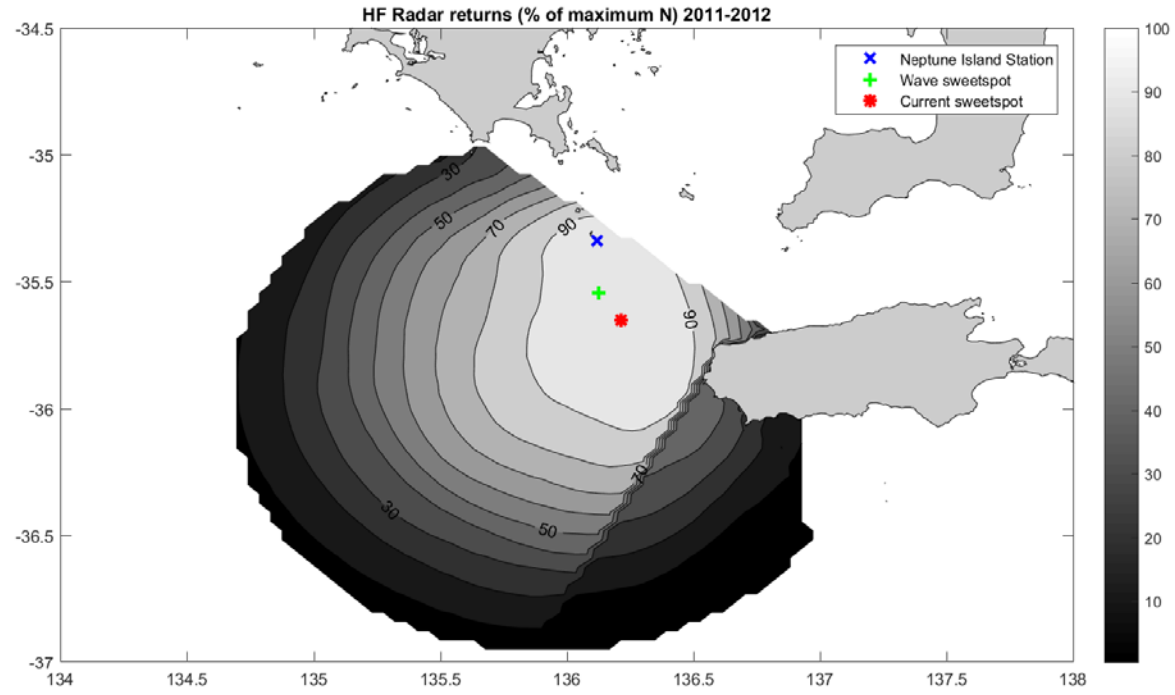

Figure 3.3.1 Coverage map of the IMOS South Australian Gulfs HF radar (SAG) Wera array.

One might think that drifters deployed as part of the Global Drifter Program (previously known as the Surface Velocity Program) would not be particularly well-suited either for measuring the effects of waves, since they are deployed with drogues centered at about 15m depth, in order to measure the average velocity of the surface mixed-layer. Indeed, one purpose of the drogues being set this deep is to minimize the effect of waves. The Stokes Drift is likely to take the drifters towards land, ending their missions. Fortunately for the present purpose, however, the GDP have recently (Lumpkin et al., 2013) revised their assessment methods of when drifters lose their drogues, finding that newer, cheaper drifters are losing their drogues much earlier than the older designs. According to the GDP (http://www.aoml.noaa.gov/phod/dac/dirall.html), all the drifters that were within the domain of our GAB models in 2011-12 had no drogue attached (in conflict with earlier determinations). Thus, we have an un-anticipated surface velocity dataset comprising 1957 drifter-days for the two years, which is nearly three active drifters on any particular day. Lacking drogues and having a significant amount of freeboard, these drifters do suffer from some

degree of wind-driven slip relative to the water. Griffin et al. (2016) found that in the Indian Ocean, the slip of undrogued drifters relative to the BRAN2015 (Oke et al. 2013a,b) 0-5m average surface water velocity was statistically indistinguishable from the WaveWatch III estimates of Stokes Drift, and equal (in the Indian Ocean) to 1.2% of the wind speed on long-term average.

BP contracted RPS-MetOcean Engineers to carry out a one-year field program from November 2011 to December 2012. Moorings MET-01 and Met-02 were in 200m and 1425m of water, respectively, at the head of the Bight (longitude 130° 39' E), at 33° 22'S and 34° 28'S. Current measurements were conducted using RPS CM04 current meters. The CM04 is a vector-averaging current meter which operates on an acoustic phase shift principle. Continuously sensed velocity components are internally rotated to a north-south, east-west coordinate system using orientation information from an internal compass. For more details see Middleton et al. (2017).

3.4 Hydrodynamic models and the butterfly effect

Ocean models, like the real ocean, are subject to chaos (the 'butterfly effect'). Infinitesimally small changes can become amplified through various instabilities. This makes it difficult to interpret experiments using ocean models, because the observed 'response' to a change of a model parameter or algorithm may be predominately a measure of the model's sensitivity to changes of any nature. To overcome this, SHOC-wave was run in a mode to suppress the chaotic behaviour by constraining the evolution of the model's temperature and salinity fields to follow those of the global model (BRAN2015) that was used for specifying the boundary and initial conditions. In this mode, spontaneous baroclinic instabilities were suppressed, but velocity gradients in the near-surface were only very weakly influenced. This approach was not taken in the experiments with COAWST however, so we will focus on COAWST-ROMS differences in relatively shallow water where baroclinic instabilities are less important and the model behaviour is much more deterministic.

4. RESULTS

4.1 SHOC-wave evaluation

Here, we compare and analyse results from just a final set of SHOC-wave model runs: Run 55, which included no wave parameterisations; and Run 53, which accounted for waves via Stokes-Coriolis, radiation stress terms, wind-stress adjustment to account for the wave supported wind stress and wave to ocean stress, and Langmuir mixing of the surface ocean (Moon 2005, Harcourt, 2012).

Figure 4.1.1 compares the SHOC-wave run 53 with drifters. The r.m.s. errors (bottom panel) for the u and v components are both 0.16 m/s. For the without-waves SHOC run 55, these values are 0.17 m/s (Figure 4.1.2), an arguably insignificant difference, but in the right direction at least. The 'traditional' (and much simpler) approach of simply adding Stokes Drift to the output of a no-waves model run yields 0.18 and 0.17 m/s (Figure 4.1.3). The maps show the greatest errors are along the shelf break, where the speeds are highest, according to both the observations and the models. Most of the total r.m.s. error, therefore, appears not to be related directly to waves, whose influence is presumably more uniformly spread across the domain.

Results for the [u, v] error of the **mean** (over all observations) velocity are also subtle: [0.006, -0.011]m/s for SHOC-waves (Figure 4.1.4), [0.008, -0.014]m/s without (Figure 4.1.5) and [0.027, 0.003]m/s (Figure 4.1.6) if Stokes Drift is simply added on without accounting for interactions via Stokes-Coriolis. Thus, the models and the drifters agree that the mean drift velocity is about 4cm/s towards the NE (see also Figure 4.1.7), and while SHOC-wave has the smallest vector error (1.5cm/s magnitude, vs 1.9cm/s for SHOC), the difference is hardly significant. What is perhaps the hardest result to explain is that the model with the greatest error of all is when the total surface drift is estimated by simply adding Stokes Drift to the standard SHOC model. We expected this to be the 2nd-best approach, not the 3rd. It contradicts the findings of Griffin et al. (2016) who did a similar analysis for a far-larger spatial domain, showing that accounting for Stokes in the 'simple' way was a definite improvement over not accounting for it at all.

Comparing the SHOC and SHOC-wave models directly with each other (rather than just where drifter observations are), we see (Figure 4.1.8) the time-averaged net result in SHOC of including waves is small (<5cm/s in most places, 1cm/s spatially averaged). The largest change is not, interestingly, where the waves are large but near the shelf break, and along the coast. The near-zero net result (in the centre of the model domain) implies the applied Stokes Drift (computed from the wave field) is being completely cancelled out by the dynamical response of the model. We anticipated this would happen, but not to this degree (e.g. see Polton 2005). This result explains why omission of the dynamical feedback (via the Stokes-Coriolis term) makes such a big difference (but not why that difference is so large).

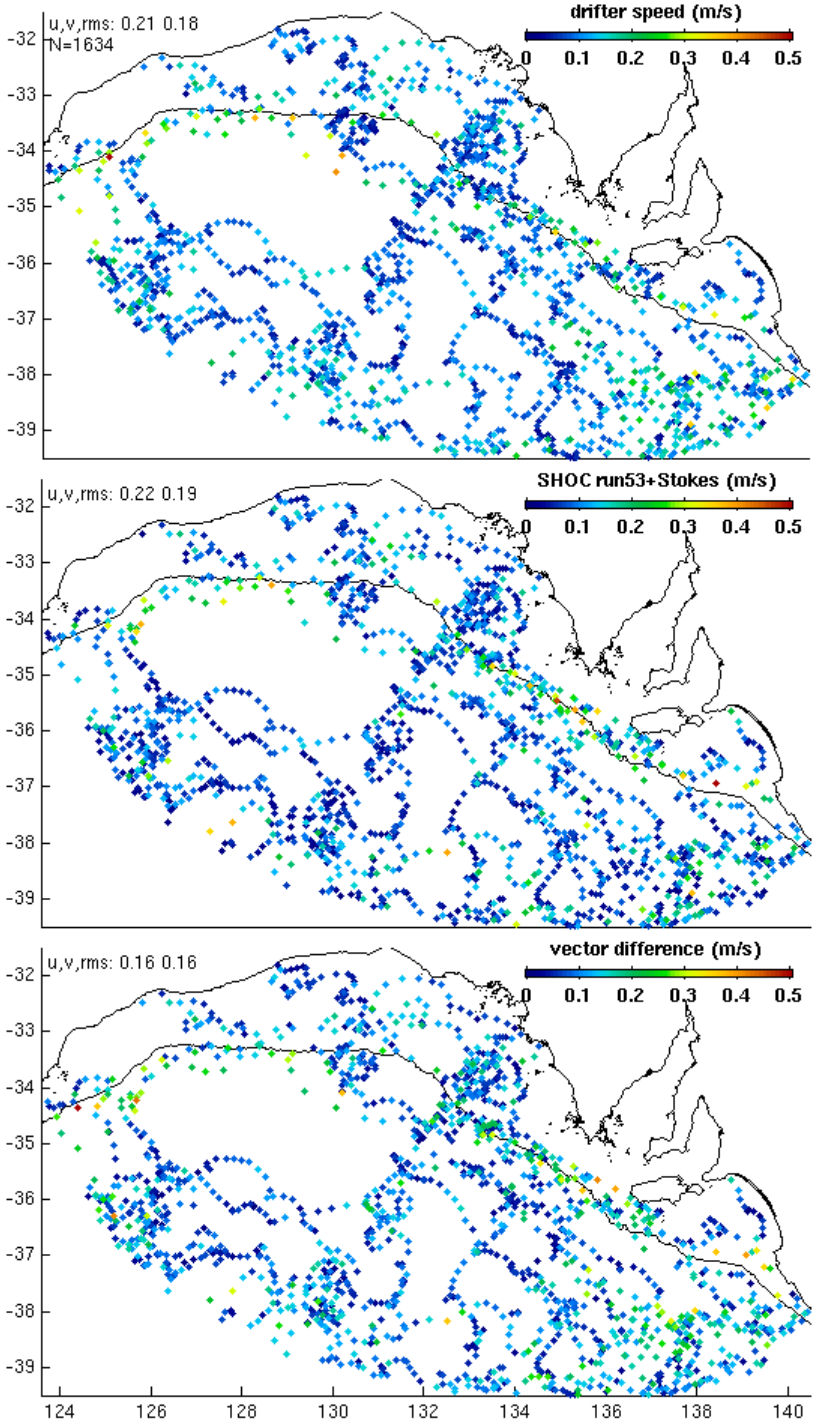

*Figure 4.1.1 Tracks of drifting buoys, colour-coded by the magnitude of the 24h-average velocity (upper panel), the **SHOC-wave** model values sampled at the place and time of the observations (middle panel) and the magnitudes of the vector model-drifter differences (lower panel). Inset values at top left of each panel list the root mean square of the u (eastward) and v (northward) components of the velocity vectors.*

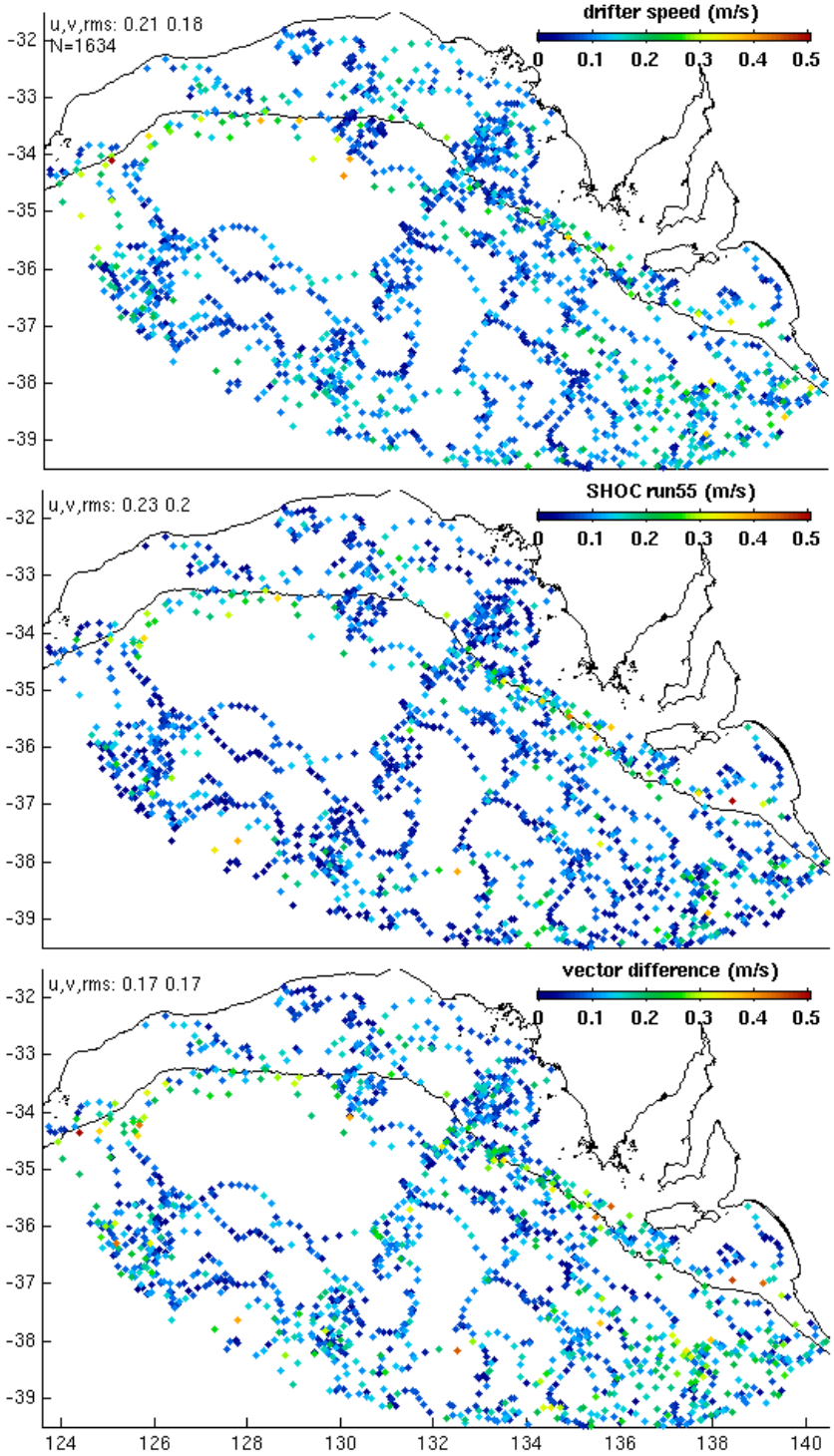

*Figure 4.1.2 Tracks of drifting buoys, colour-coded by the magnitude of the 24h-average velocity (upper panel), the SHOC model (**no waves**) values sampled at the place and time of the observations (middle panel) and the magnitudes of the vector model-drifter differences (lower panel). Inset values at top left of each panel list the root mean square of the u (eastward) and v (northward) components of the velocity vectors.*

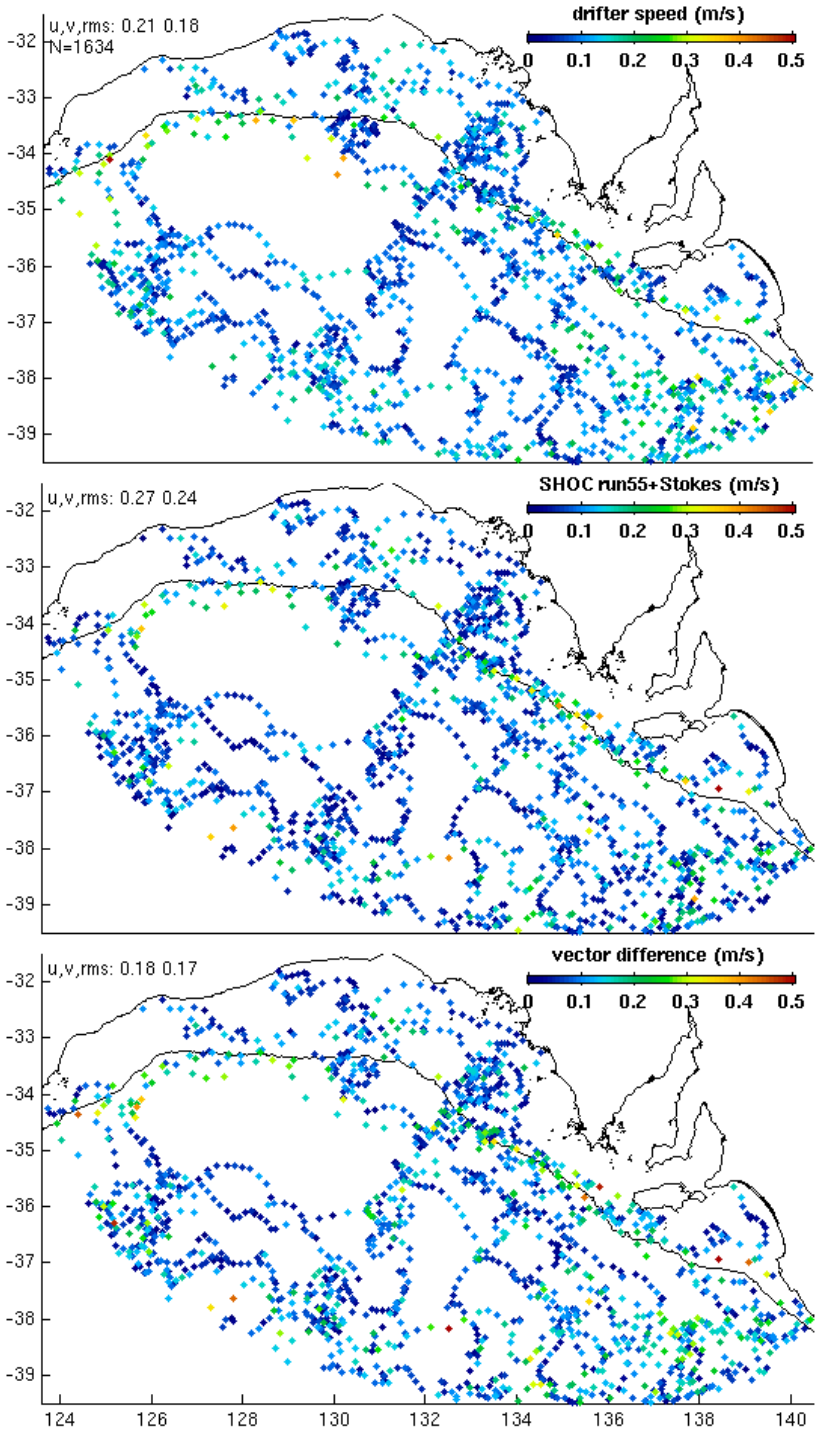

*Figure 4.1.3 Tracks of drifting buoys, colour-coded by the magnitude of the 24h-average velocity (upper panel), the SHOC model (**with Stokes added independently**) values sampled at the place and time of the observations (middle panel) and the magnitudes of the vector model-drifter differences (lower panel). Inset values at top left of each panel list the root mean square of the u (eastward) and v (northward) components of the velocity vectors.*

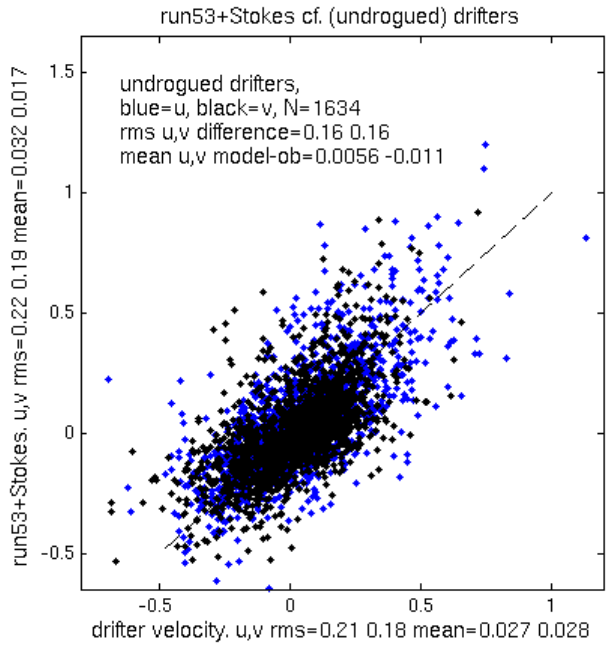

Figure 4.1.4 ***SHOC-wave*** *surface velocity eastward (blue) and northward (black) components (uppermost 0.5m-thick layer) vs drifter velocity. The dashed line is 1:1, not a line of best fit. Drifter and model (sampled at drifter locations) velocity statistics (u,v mean and r.m.s.) are listed in the axis labels. Drifter-model difference statistics are inset.*

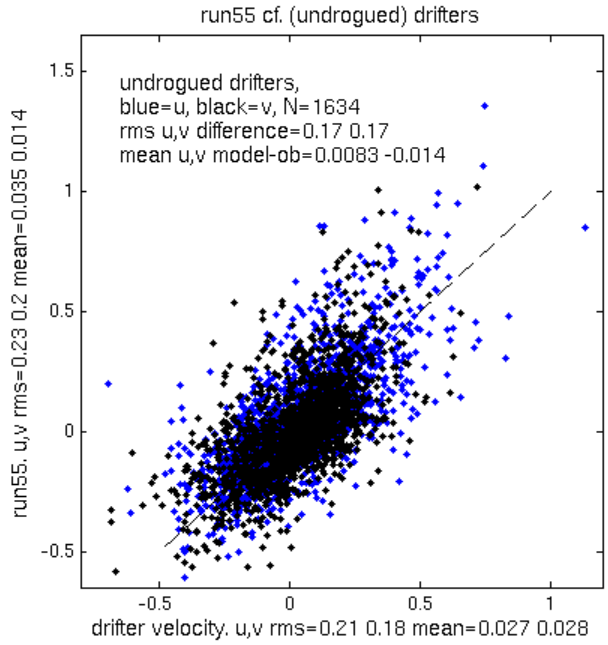

Figure 4.1.5 ***SHOC (no waves)*** *surface velocity (uppermost 0.5m-thick layer) vs drifter velocity. The dashed line is 1:1, not a line of best fit.*

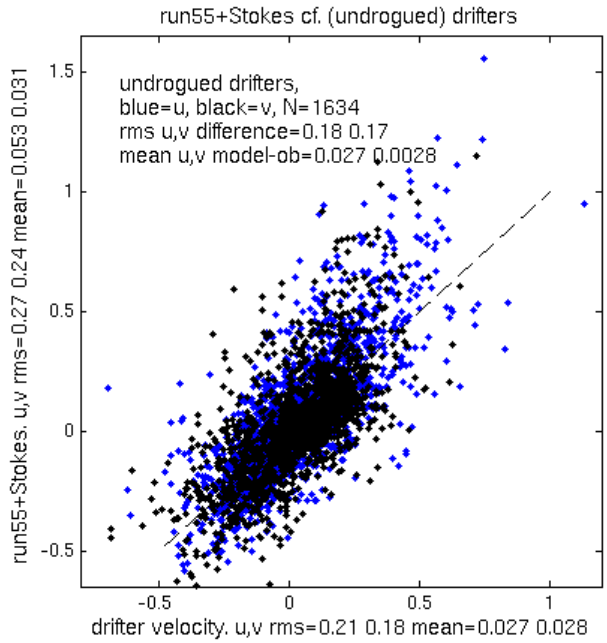

Figure 4.1.6 ***SHOC (+ independent Stokes)*** *surface velocity (uppermost 0.5m-thick layer) vs drifter velocity. The dashed line is 1:1, not a line of best fit*

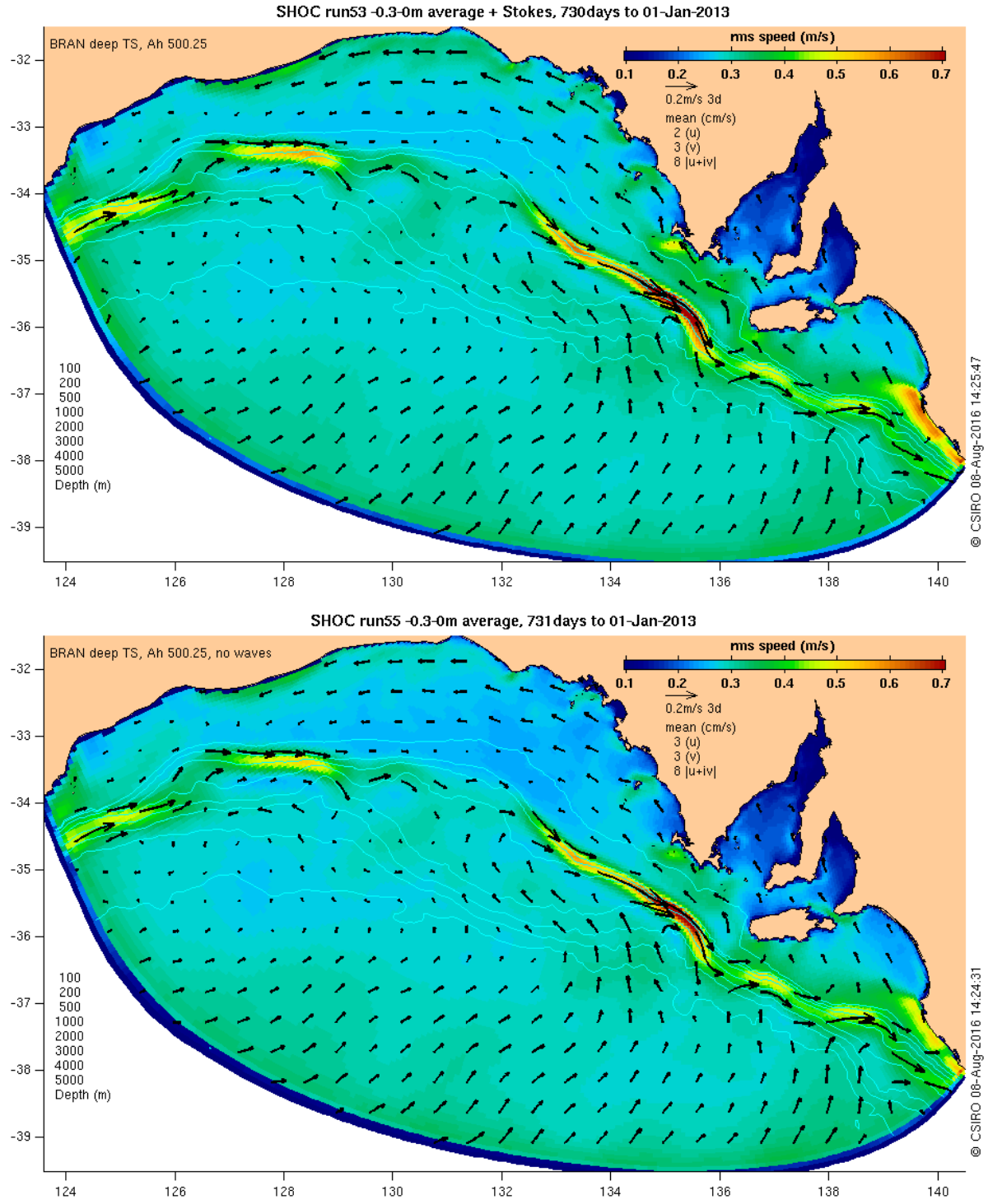

Figure 4.1.7 Two-year mean of the total surface velocity estimated by SHOC-wave (upper) and SHOC (lower).

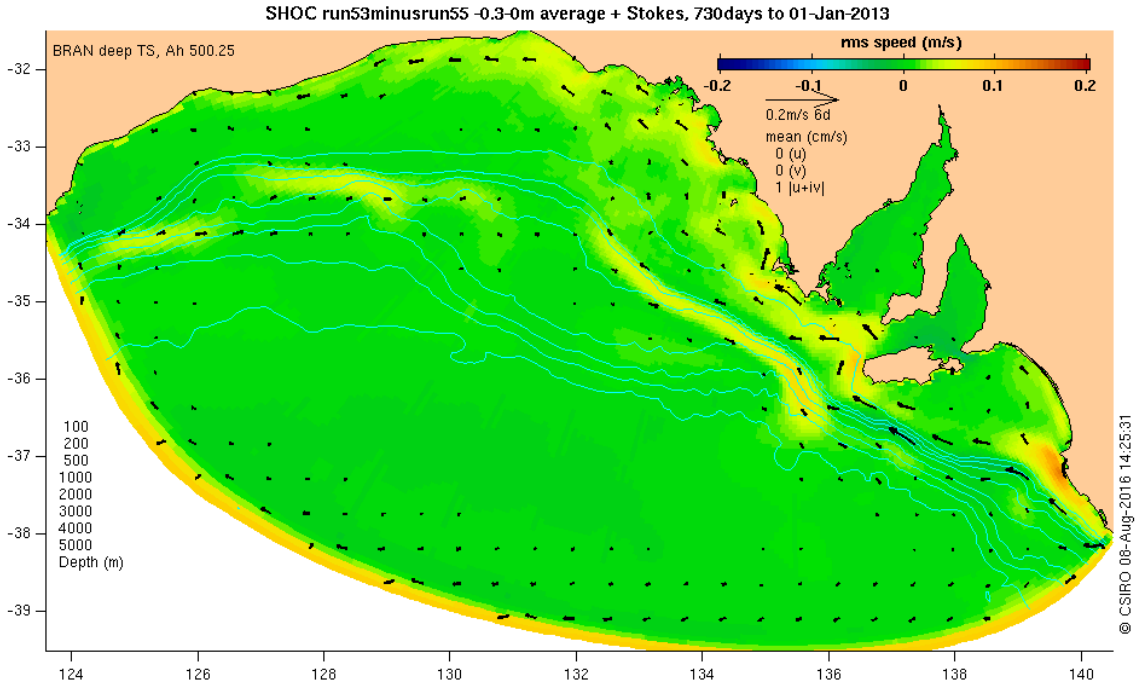

Figure 4.1.8 Difference of the two-year means of the total surface velocity estimated by SHOC-wave and SHOC. Vectors: SHOC-wave minus SHOC mean surface velocity. Colour-fill: SHOC-wave minus SHOC difference of the r.m.s. speeds (not the r.m.s. of the difference).

4.2 SHOC-wave 2011-12 simulation

In addition to the model experiment described above, SHOC-wave was also run in 'free' mode without any interior nudging of the temperature and salinity fields to BRAN2015. Of all the SHOC runs, this one agreed best with the temperatures observed at the BP shelf edge mooring (Figure 4.2.1). But this better agreement is just an example of the butterfly effect mentioned above: in this model run, the Leeuwin Current developed then shed an anticyclonic eddy near the mooring sites in mid-2012 (Figure 4.2.2), taking Leeuwin Current water farther offshelf than at the same time in the without-waves run. The link between Stokes Drift and eddy formation is extremely indirect, so there is no basis to credit the improved agreement with the observations at M1 to the inclusion of waves, in this case.

We will not further describe the results here because they are very similar to the without-waves SHOC results reported by Middleton et al. (2017).

Readers can browse the online archives of model results of both the with-waves and without-waves models. The archives include, for example, maps of the average surface and near-surface velocity for early 2011 (Figure 4.2.3), mid 2011 (Figure 4.2.4), and other layers, quantities, subsequent seasons and other time-averaging intervals.

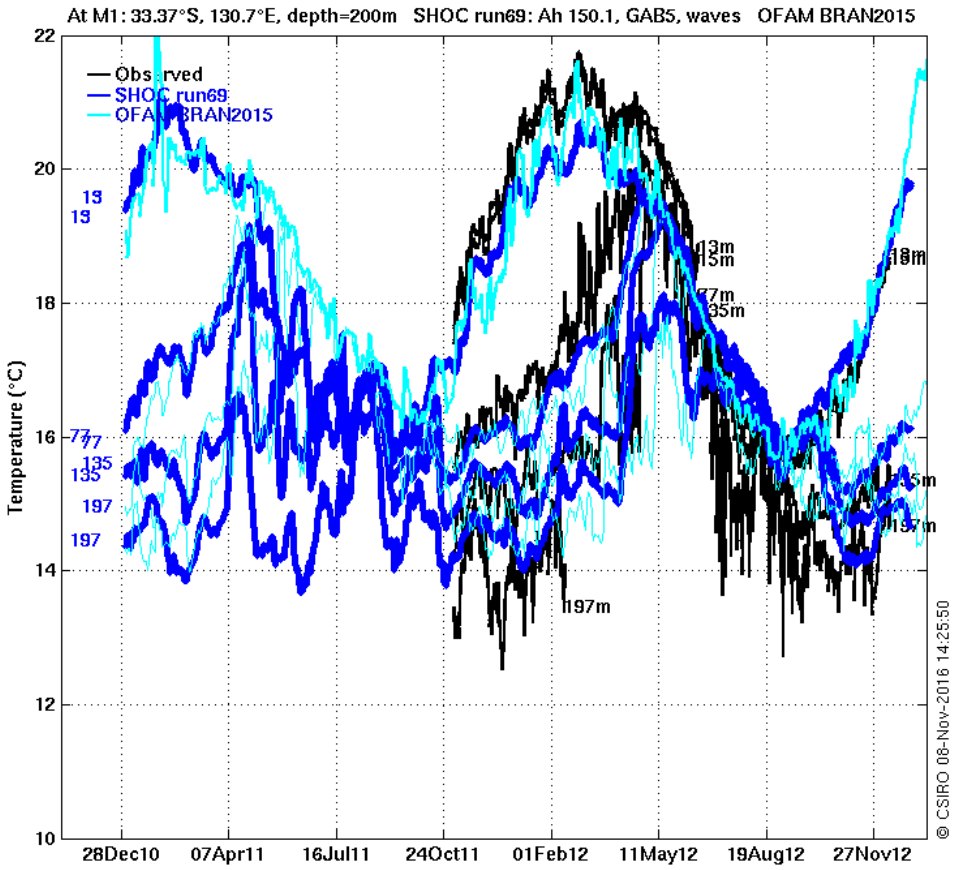

Figure 4.2.1 Temperature time series at the location of the BP M1 mooring at the 200m isobath at the head of the Bight (130.5°E), for 2011-12. The in-situ observations are in black, SHOC-wave run 69 is dark blue while the BRAN2015 estimates are in faint blue. [online copy] [same but without waves]

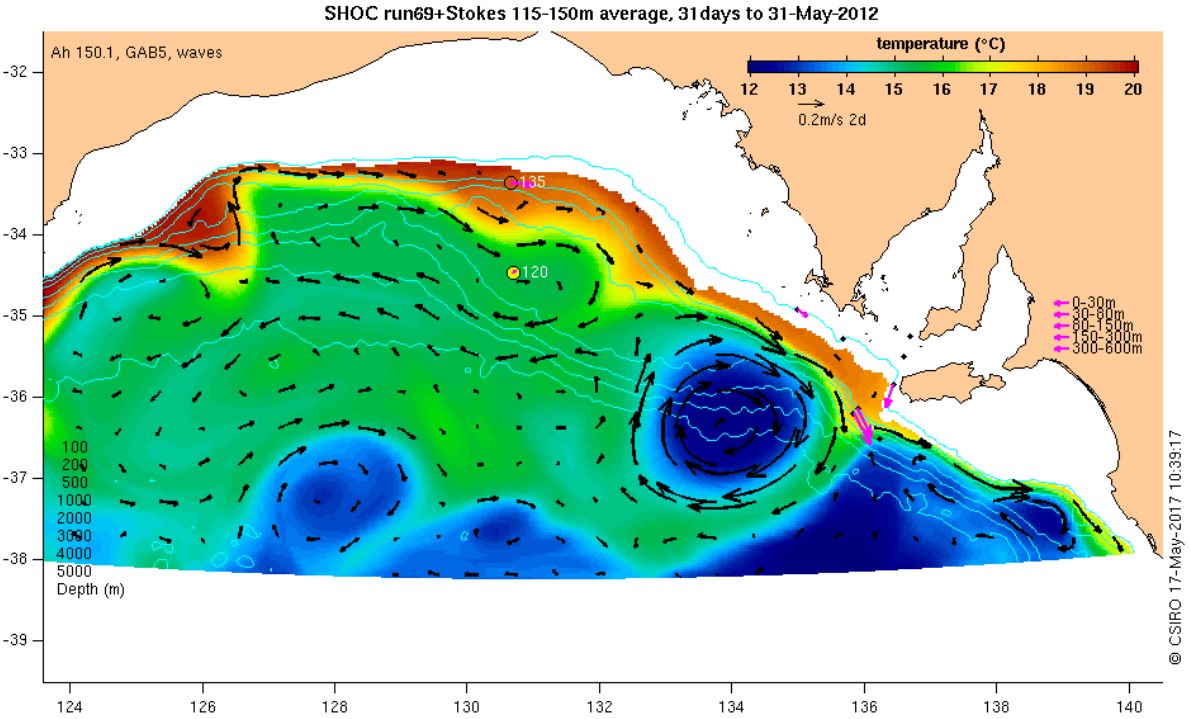

Figure 4.2.2 Sub-surface (115-150m average) temperature and velocity, averaged over May 2012, according to SHOC-wave run 69. [online copy] [same but without waves]

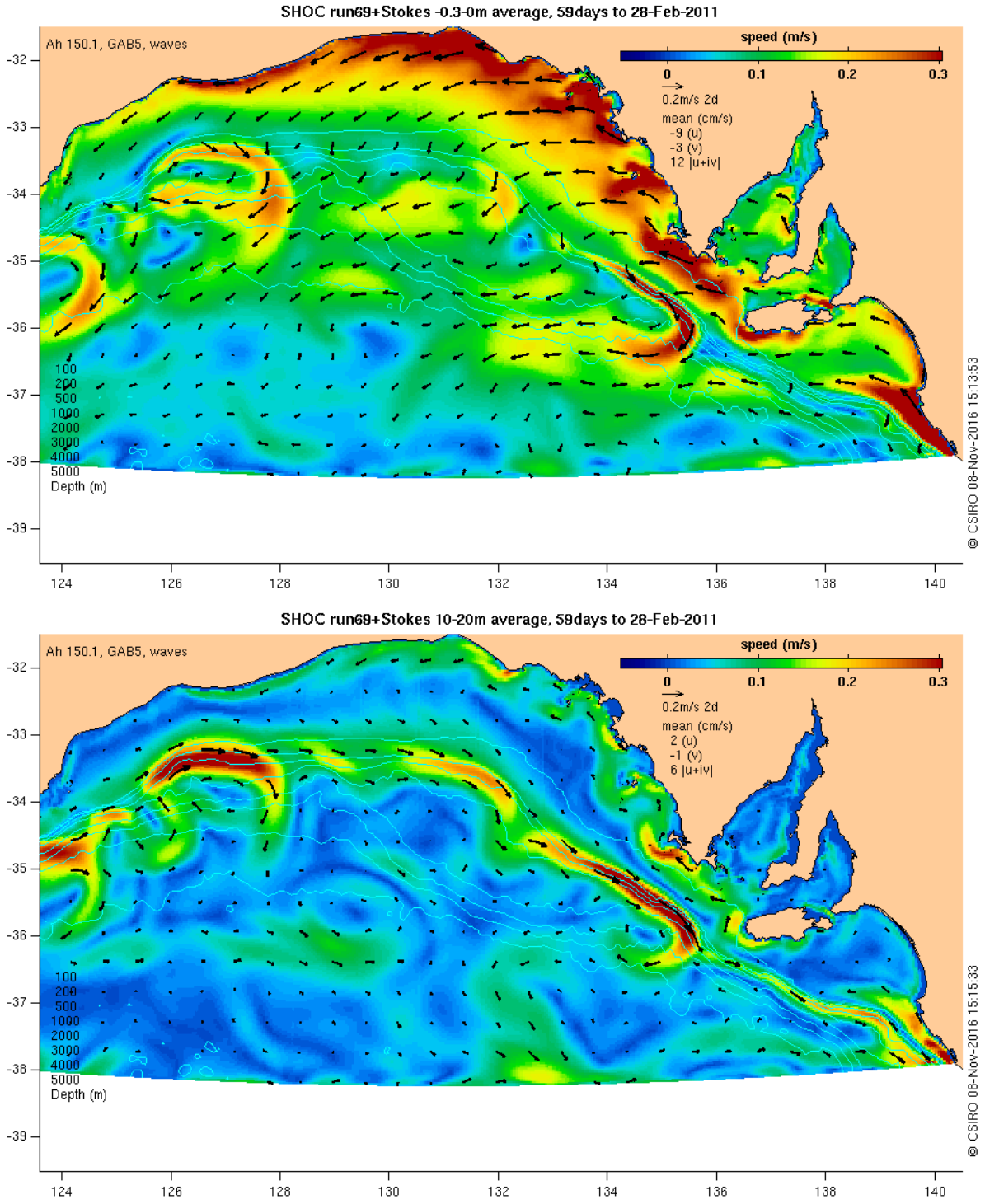

*Figure 4.2.3 Total surface velocity (Eulerian + Stokes, upper) and deeper near-surface (10-20m average, lower) velocity, averaged over **January and February** 2011, according to SHOC-wave run 69. [online copy] [same but without waves]*

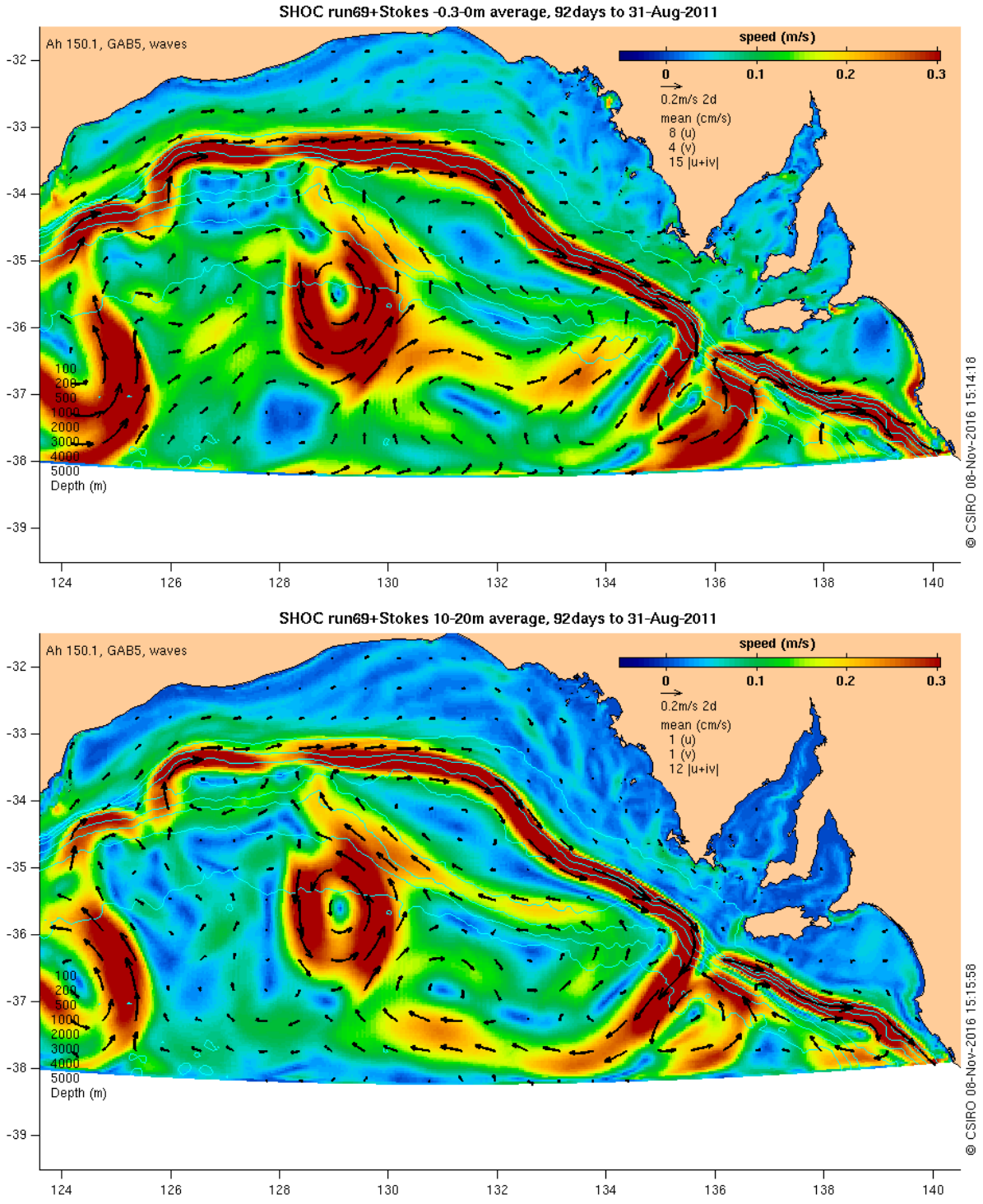

*Figure 4.2.4 Total surface velocity (Eulerian + Stokes, upper) and deeper near-surface (10-20m average, lower) velocity, averaged over **June-August** 2011, according to SHOC-wave run 69. [online copy] [same but without waves]*

4.3 COAWST

The COAWST (with-waves) and ROMS (no waves) model estimates of the near-surface (0-5m) current at the centre of the SAG radar coverage (Figure 3.3.1) both compare quite well with the radar observations (Figure 4.3.1). The difference between the two models on any one day can be significant but the r.m.s. differences from the observations are essentially the same for the COAWST (0.08, 0.08, 0.09, 0.09m/s for u, v 2011 and u, v 2012) and ROMS (0.08, 0.08, 0.10, 0.08m/s) runs of the model, suggesting little if any net detectable benefit from the inclusion of wave information in the model.

Similarly, comparison of temperature observations at the two BP moorings with COAWST and ROMS (Figure 4.3.2) shows occasionally-large differences between the two models at the observation locations, but no clear tendency for either model to be closer to the data.

Comparing the COAWST and ROMS models directly with each other (and at the surface, rather than near-surface, and just at the mooring and radar sites), we see the estimated long-term mean total surface current (Figure 4.3.4) is much more strongly uniformly directed onshore when the waves are taken into account, especially over the continental shelf where large energetic eddies are absent. This is in contrast to the results from SHOC-wave, where the addition of Stokes Drift was completely cancelled out by the Stokes-Coriolis dynamics.

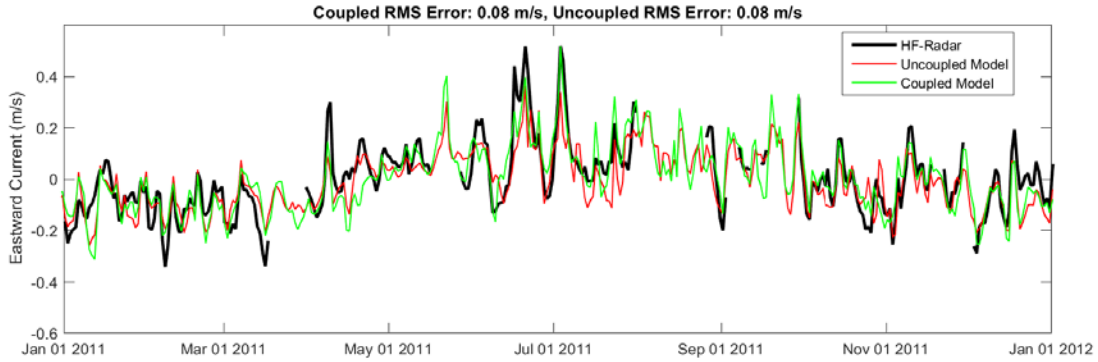

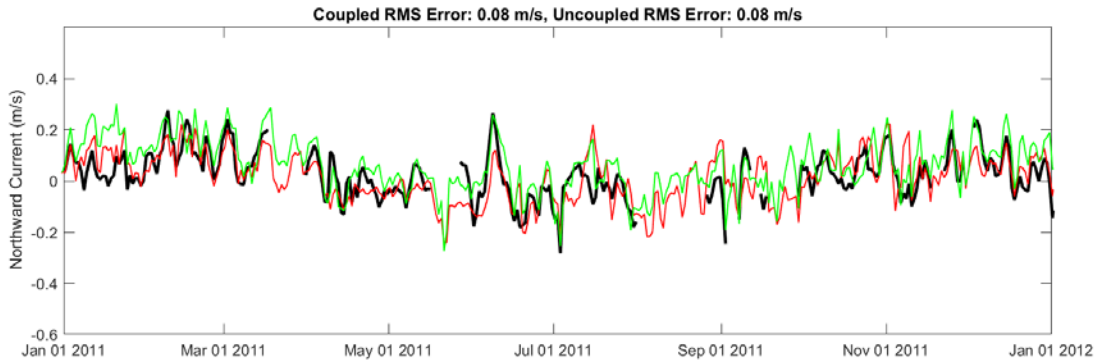

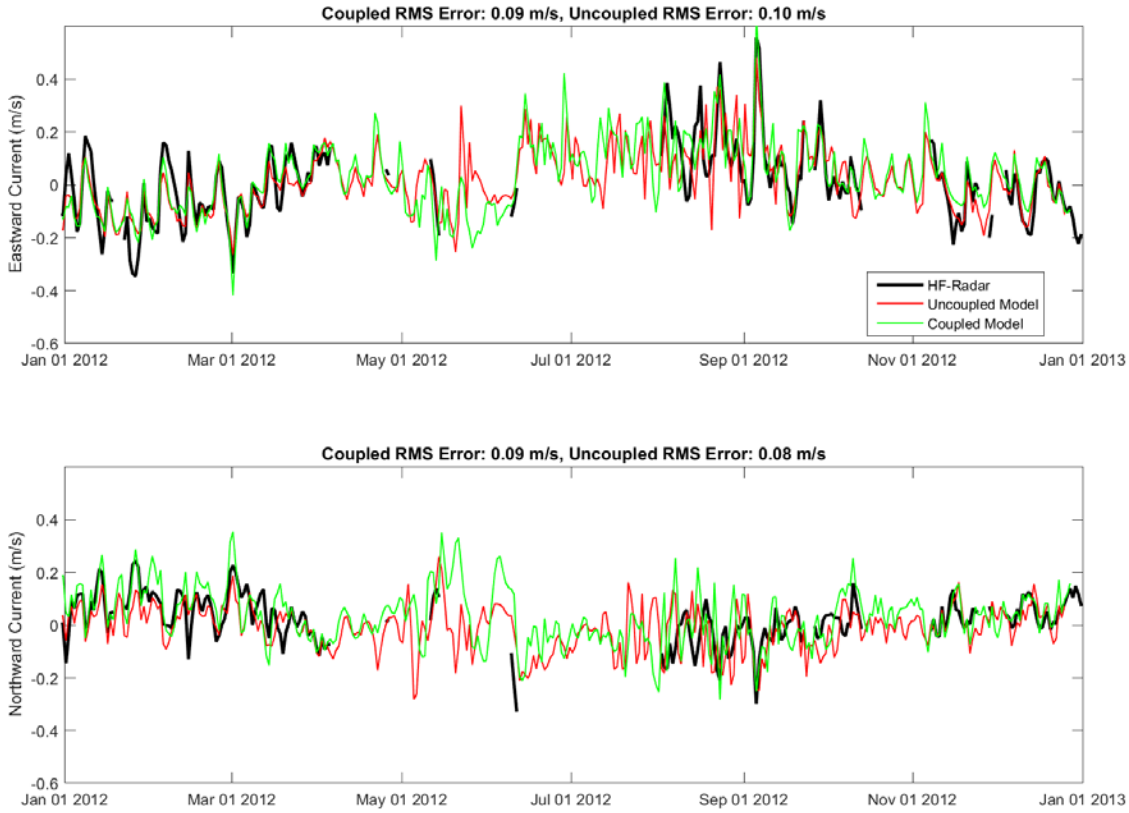

Figure 4.3.1 Radar eastward and northward velocities for 2011 (two upper panels) and 2012 (two lower panels) compared with two model estimates: COAWST (green, with waves) and ROMS (red, without waves).

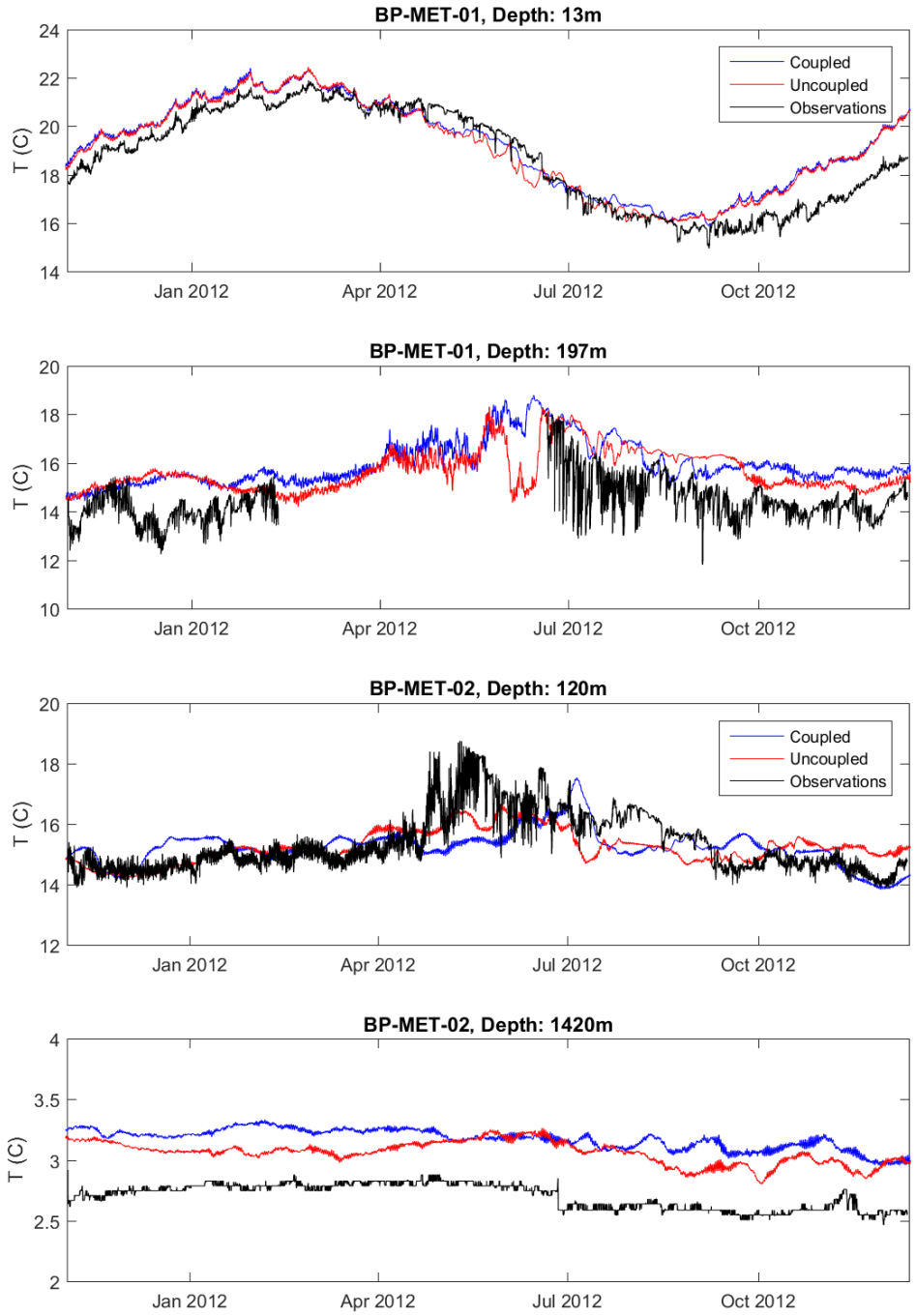

Figure 4.3.2 Temperature observations by the shallowest and deepest instruments at the BP MET-01 (200m water depth) and MET-02 (1450m) mooring sites compared with two models estimates: COAWST (blue, with waves) and ROMS (red, without waves).

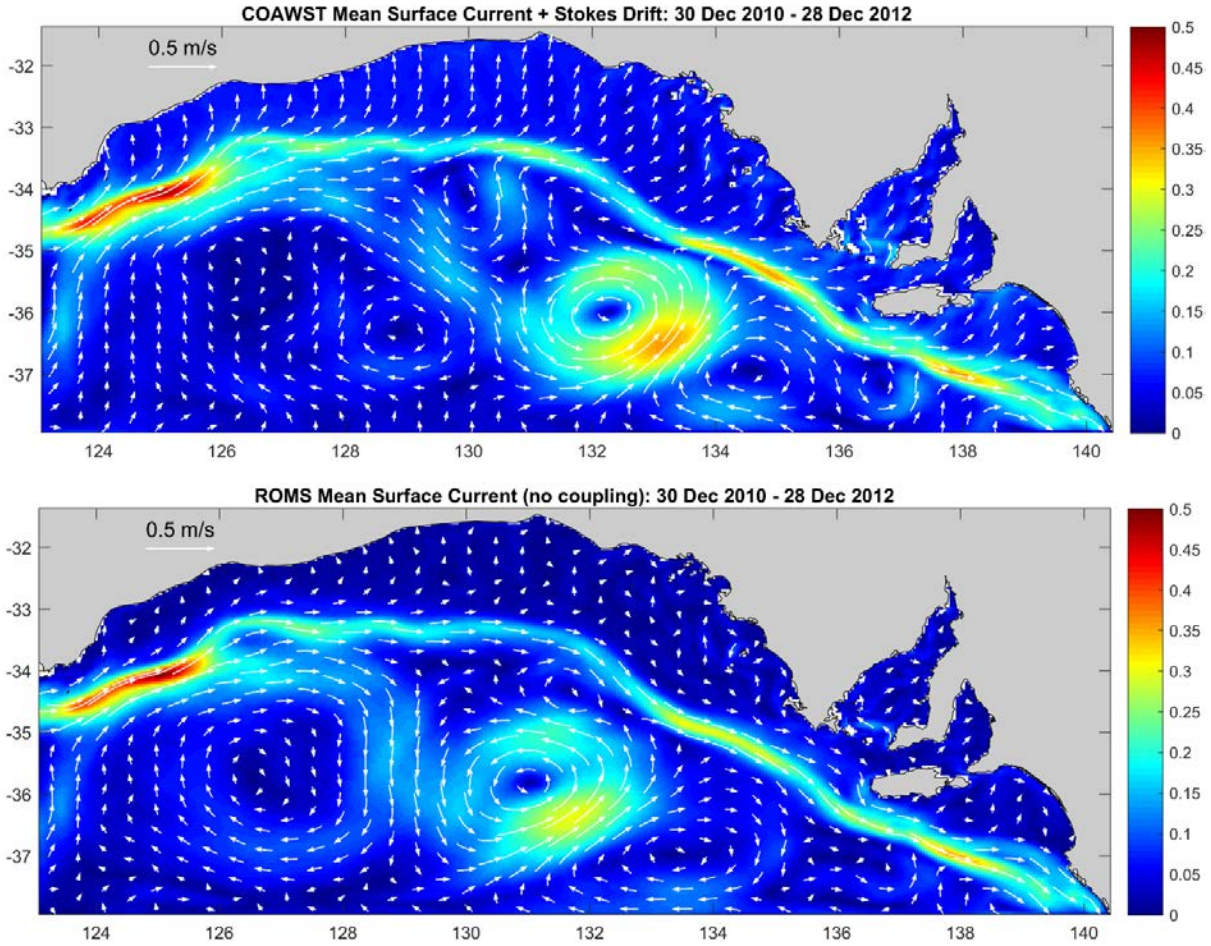

Figure 4.3.3 2011-2012 average of total surface currents (including Stokes drift for COAWST) for COAWST (upper) and ROMS (lower).

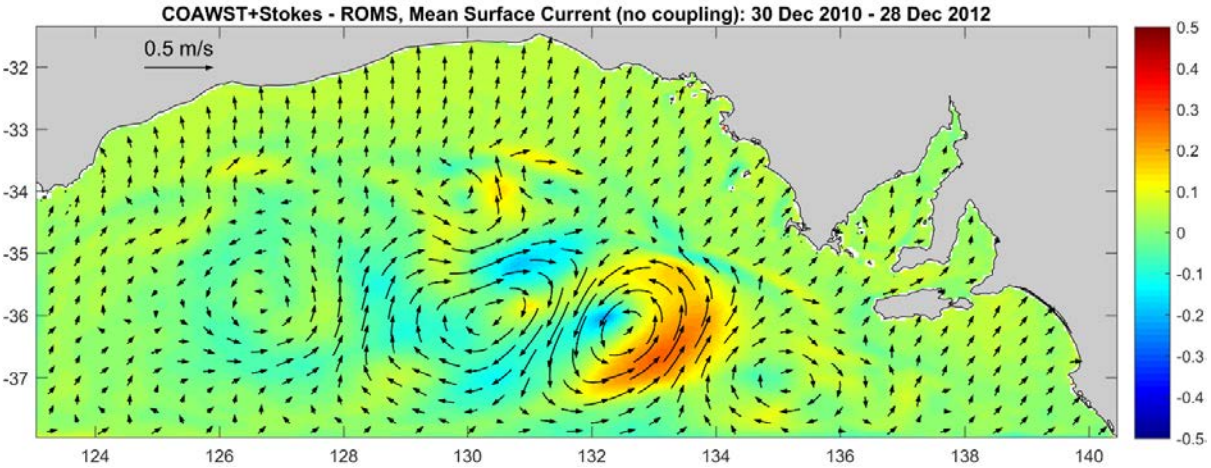

Figure 4.3.4 2011-2012 COAWST-ROMS difference of total surface current (equivalent to Figure 4.1.8 for SHOC-wave - SHOC).

4.4 Stokes Drift

To try and understand why the SHOC-wave and COAWST models were yielding such different surface current responses to the inclusion of wave forcing, we started by taking a closer look at how the two modelling systems were estimating the Stokes Drift from the wave information.

Sections 3.1 and 3.2 list the quantities passed between the model components. In the SHOC-wave system, the Stokes Drift is estimated within the NOAA WaveWatchIII model, from the full directional wave spectrum. This yields an estimate that has a strong seasonal cycle, varying, for example, from 10cm/s northwestward in February 2011 to 5cm/s eastward in August 2011 (Figure 4.4.1).

The near-surface Stokes Drift is predominately due to wind-sea - the contribution from swell is small, as shown (in blue) in Figure 4.4.1. This is because the Stokes Drift

$$u_S(z) = \int_0^{2\pi} \int_0^{\infty} ck^2 \psi(f,\theta) \exp(2kz) \cos\theta \, df \, d\theta,$$

(Moon 2005, equation 17) depends on the third power of the frequency (after substituting the deep water dispersion relation). The seasonal variability of the full-spectrum Stokes Drift therefore mimics the seasonal cycle (Figures 3.1.1 and 3.1.3 of Middleton et al. 2017) of the wind.

THE COAWST estimates of the 2011-2012 mean February and August surface Stokes Drift have similar magnitudes to the WaveWatchIII estimates, at about 6cm/s. The seasonal change in direction, however, is only about 45° (compared to the 135° in WaveWatchIII). The COAWST direction is much more consistently towards the shore (Figure 4.4.2). This is because COAWST estimates the Stokes drift from the direction, period and height of the spectral peak, which is usually in the swell band, and consistently to the NE in the GAB (Figure 2.1.1). This method is clearly only an approximation of the full calculation, but at least it does produce a fairly reasonable estimate.

There is no way to actually observe the Stokes Drift in isolation of other contributions to the total surface drift. But we can verify that the modelled directional wave spectrum is close to the spectrum observed by the SAG radar, as shown in he left panels of Figure 4.4.4. The right panels show how the spectral contributions to the Stokes Drift compare, while the integrated value is listed at the top. For this April-Sept 2011 period, the SWAN full-spectrum (to 5s period) estimate of the surface Stokes velocity is 2.9cm/s at 34°T. The estimate from the radar is 30% (1cm/s) less, at 1.8cm/s at 31°T, giving some confidence that the basis of the wave model's estimate of the Stokes Drift is fairly sound, if the whole spectrum is used.

These results show that while the WAVEWatchIII+SHOC and SWAN+ROMS systems are yielding fairly similar estimates of the Stokes Drift, there are significant differences, presumably due to the simplified approach taken in the latter system. We think a very worthwhile improvement to the COAWST system would be to pass the Stokes Drift velocities from SWAN to ROMS, rather than just the bulk wave parameters from which only an approximation of the Stokes drift can be calculated.

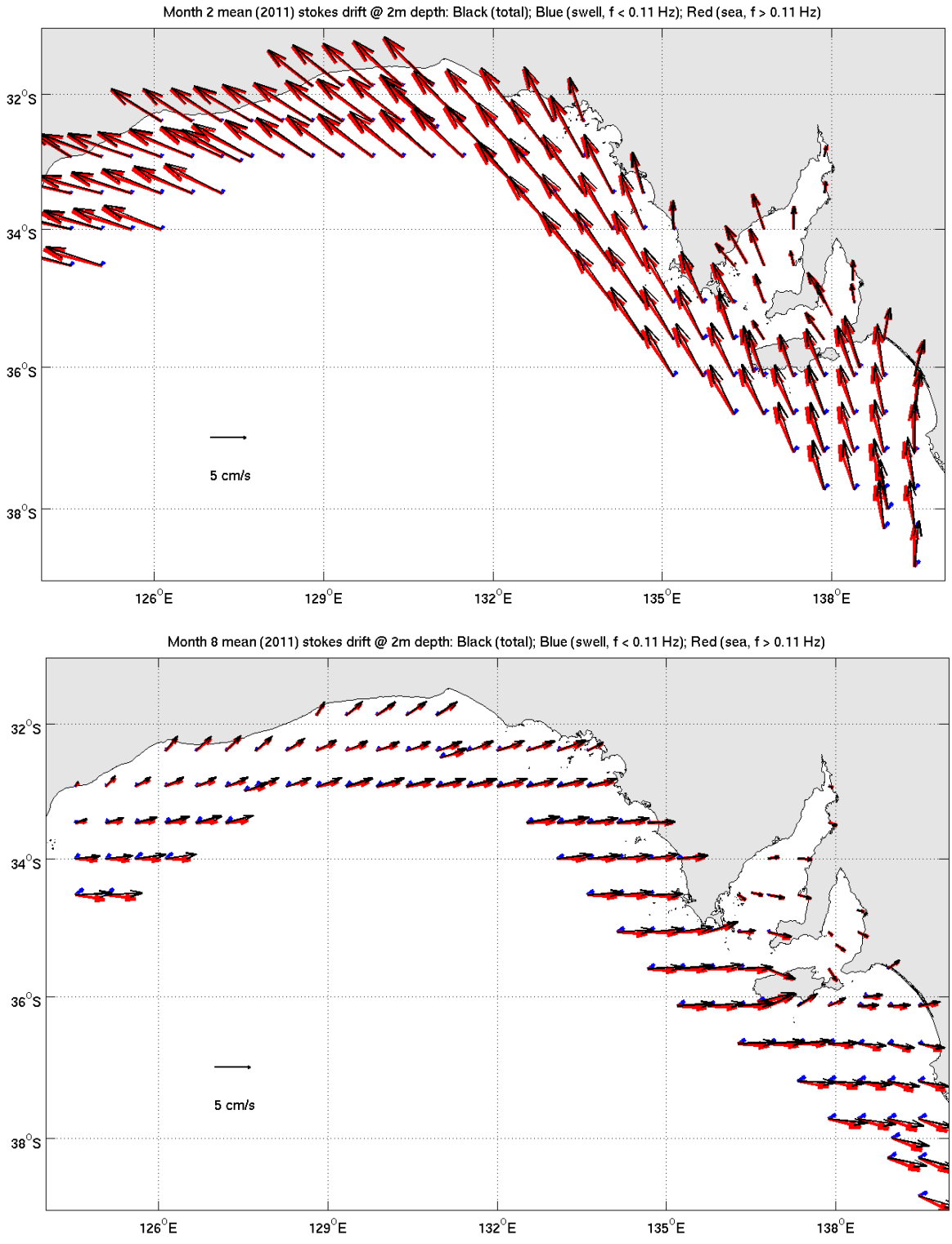

Figure 4.4.1 February 2011 (upper) and August 2011 (lower) Stokes Drift velocities at 2m depth, estimated from the CAWCR Wavewatch III waves hindcast directional spectrum. Contributions from swell (blue) and wind-sea (red) are shown separately. Estimates for other months are available [online].

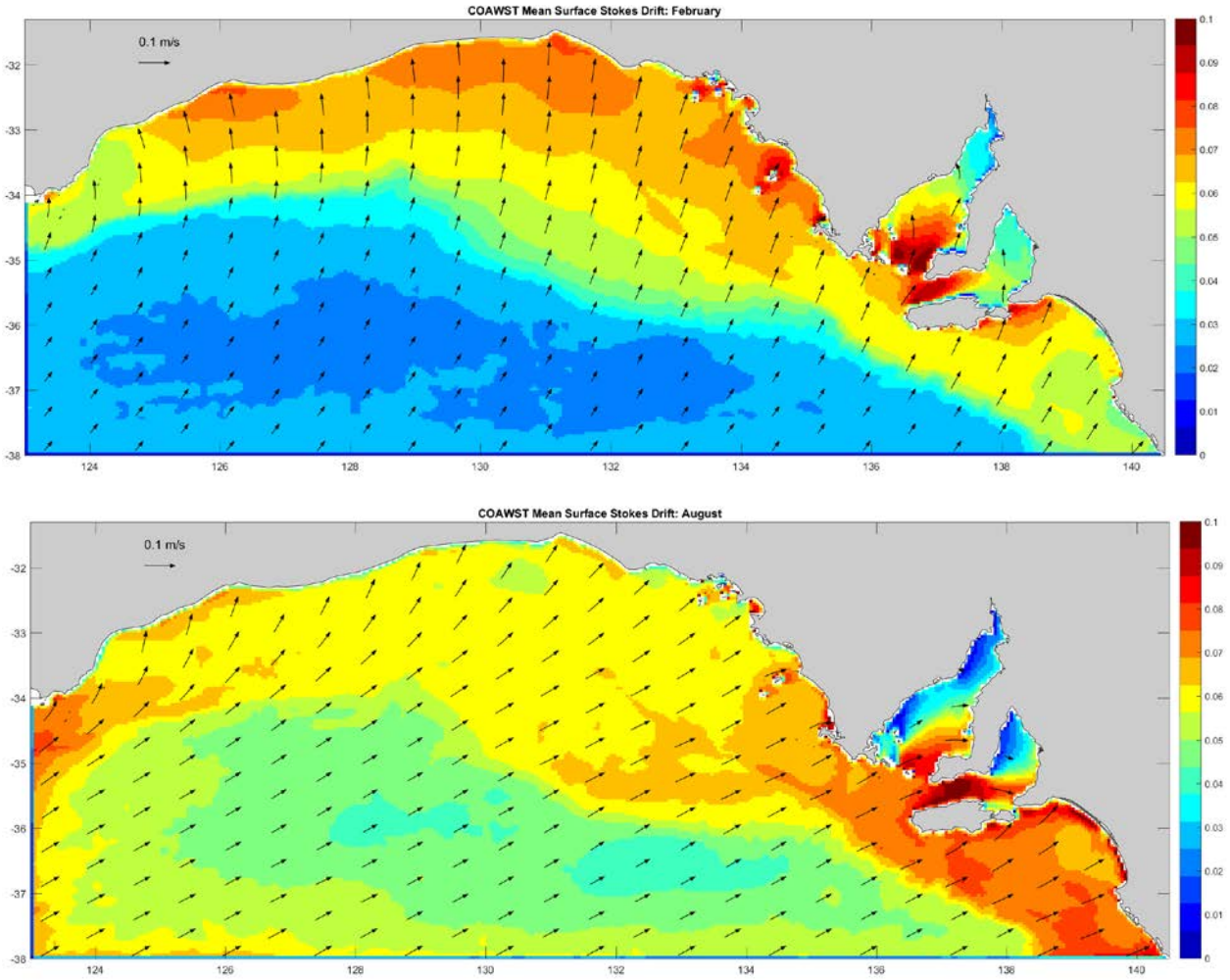

Figure 4.4.2 February (upper) and August (lower) 2011-2012 average of surface Stokes Drift calculated by COAWST from the significant wave height, period and direction. Estimates for other months are available [online].

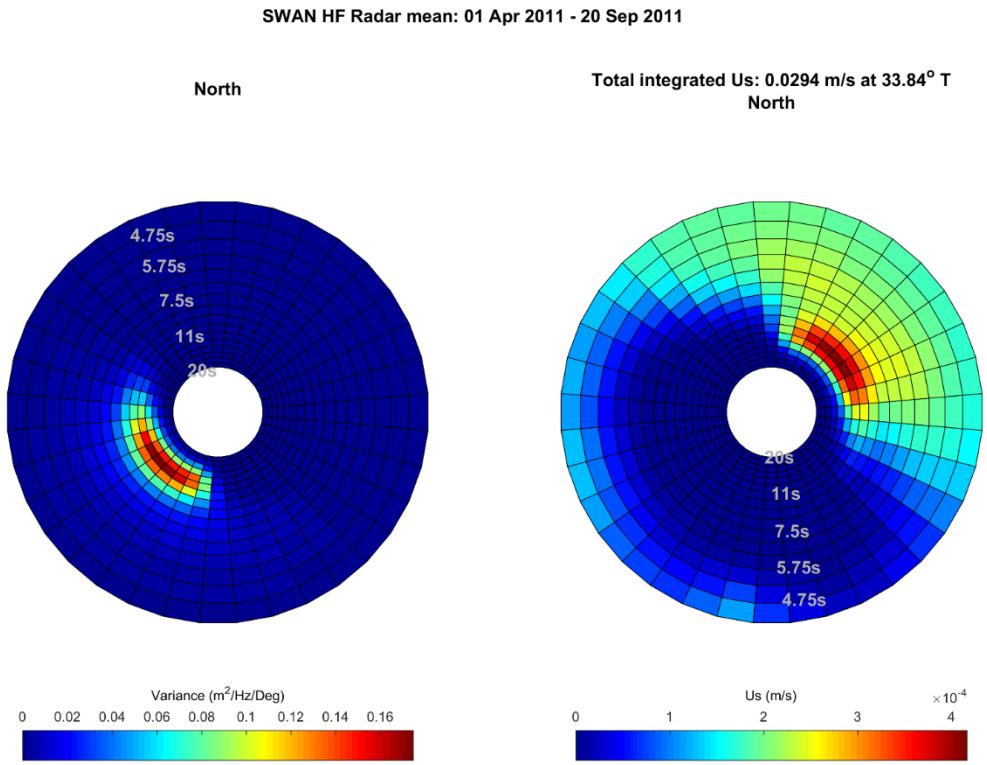

Figure 4.4.3 Winter 2011 averaged directional wave spectrum (as direction-from) estimated by the SWAN component of COAWST (left) and the associated spectral components of the derived Stokes drift (right), at the location of the IMOS SAG HF radar.

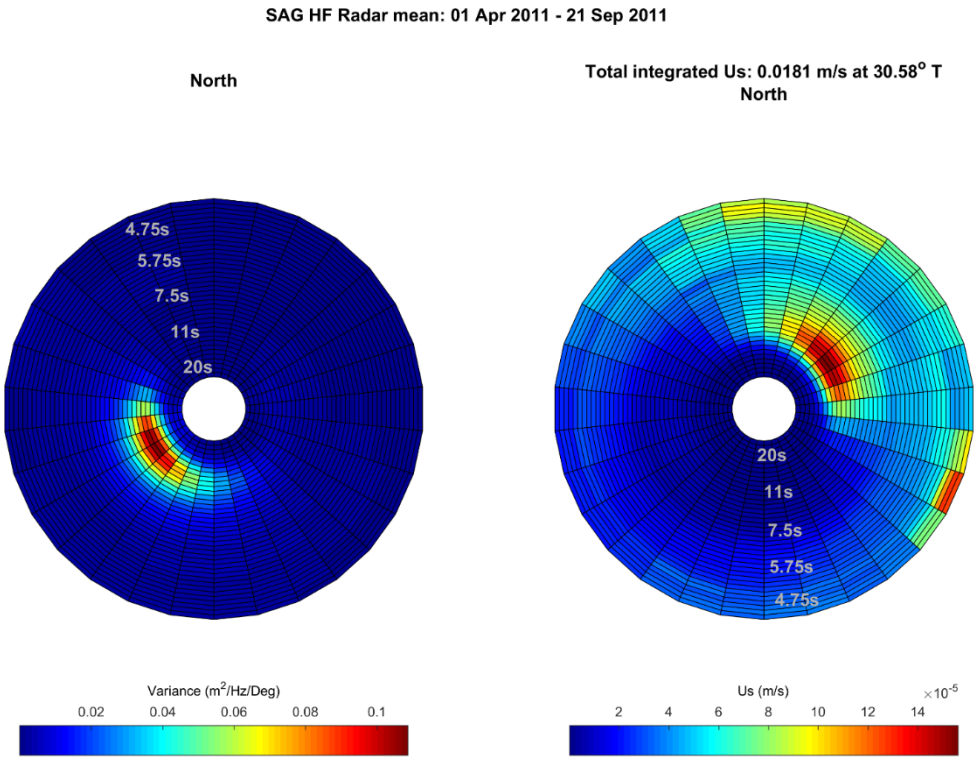

Figure 4.4.4 IMOS SAG HF radar observations of the winter 2011 directional wave spectrum (as direction-from) (left) and the associated spectral components of the derived Stokes drift (right).

5. DISCUSSION

Our analysis of the way the two modelling systems arrive at estimates of the Stokes Drift highlighted the fact that the COAWST approach makes an approximation that seems to us to be unnecessary. An obvious improvement is to calculate the depth-dependent Stokes Drift within the wave model and pass this to the circulation model. This would be a relatively easy way of making a small but significant improvement. The WavewatchIII+SHOC system goes halfway towards this, by calculating the surface value of the Stokes Drift. Calculating values at a number of depths would be better than assuming a decay rate based on the period of the spectral peak.

The much harder question is why the two hydrodynamic models respond so differently to the addition of Stokes Drift as an external forcing. The Moon (2005) and Uchiyama (2010) formulations that have been implemented in SHOC and ROMS, respectively, are very similar, except for omission by Moon (2005) of the Stokes Drift in the tracer advection equation where its impact is arguably very small. We expect that further investigation of the two systems will discover why they have behaved differently so far. It is harder to anticipate if it will become clear what the correct formulation is. The lack of consensus among workers in this field (Appendix 5: Review of Wave-Ocean coupling) suggests that a solution is not around the corner.

6. CONCLUSION

The mesoscale eddies in the GAB, while certainly being much weaker than in neighbouring regions, are still strong enough to largely mask the differences between models that do and don't explicitly include representations of the many roles that waves undoubtedly have in coupling the atmosphere and the ocean. This was exacerbated by the models' tendency to generate eddies that were more energetic than are observed, and also by a negative feedback to the inclusion of Stokes Drift, in the form of an Eulerian return flow that reduces (or cancelled in the case of SHOC) the surface Lagrangian velocity.

We identified an improvement that could be made to the COAWST system (and believe the developers have independently identified this already but not yet released a version of the model with the improvement included). The implementation of the coupling formulation in SHOC requires further testing.

The only quantity that appears to be substantially influenced by taking waves explicitly into account is the time it takes buoyant matter to be transported from offshore regions to the coast. This is of interest to Theme 5 (buoyant matter only) and is also possibly relevant to explaining the lifecycle of Southern Rock Lobster (Bruce et al., 2007).

7. REFERENCES

Ardhuin FL, Marié N, Rascle N, Forget P, Roland A (2009) Observation and estimation of Lagrangian, Stokes and Eulerian currents induced by wind and waves at the sea surface. *Journal of Physical Oceanography* **39(11)**, 2820-2838.

Bruce B, D Griffin and R Bradford (2007). Larval transport and recruitment processes of southern rock lobster. Final report to FRDC project 2002/007. ISSN 1921061014. [available online].

Durrant, T., D. Greenslade, M. Hemer and C. Trenham (2014). A global wave hindcast focussed on the Central and South Pacific. CAWCR Technical Report No 70. 54p. http://www.cawcr.gov.au/technical-reports/CTR_070.pdf

Durrant, Thomas; Hemer, Mark; Smith, Grant; Trenham, Claire; Greenslade, Diana (2015): CAWCR Wave Hindcast extension June 2013 - July 2014. v1. CSIRO. Data Collection. http://doi.org/10.4225/08/55C99193B3A63

Ghantous, M. and A.V. Babanin **(2014)** One-dimensional modelling of upper ocean mixing by turbulence due to wave oribital motion. *Nonlin. Processes Geophys.*, 21, 325-338, doi:10.5194/npg-21-325-2014

Griffin, DA, Oke, PR and Jones, EM (2016). The search for MH370 and ocean surface drift. CSIRO Oceans and Atmosphere, Australia. Report number EP167888. 8 December 2016. DOI: 10.4225/08/5892224dec08c

Hemer MA and DA Griffin (2010). The wave energy resource along Australia's southern margin. Journal of Renewable and Sustainable Energy **2**, 043108 (2010); doi:10.1063/1.3464753.

Hemer, M.A., S. Zieger, T. Durrant, J. O'Grady, R.K. Hoeke, K.L. McInnes and U. Rosebrock, 2016. A revised assessment of Australia's national wave energy resource. Renewable Energy, http://dx.doi.org/10.1016/j.renene.2016.08.039

Jones, N.L., Monismith, S.G. (2008) Modelling the influence of wave-enhanced turbulence in a shallow tide- and wind-driven water column. *J. Geophys. Res.*, 113, C03009, doi:10.1029/2007JC004246.

Kumar N, Voulgaris G, Warner JC, Olabarrieta M (2012) Implementation of the vortex force formalism in the coupled ocean–atmosphere–wave–sediment transport (COAWST) modeling system for inner shelf and surf zone applications. Ocean Model 47:65–95. doi:10.1016/j.ocemod.2012.01.003

Lumpkin R, Grodsky SA, Centurioni L, Rio MH, Carton JA, Lee D (2013). Removing spurious low-frequency variability in drifter velocities, *Journal of Atmospheric and Oceanic Technology* **30**, 353-360. doi: JTECH-D-12-00139

Middleton, JF, Griffin D, Luick J, Herzfeld M, James C and Oke P (2017). Physical Oceanography of the Great Australian Bight: the science that underpins. Final Report GABRP Project 1.1. Great Australian Bight Research Program, GABRP Research Report Series Number 20, 109pp.

Moon, I-J. (2005) Impact of a coupled ocean wave–tide–circulation system on coastal modeling. Ocean Modelling 8, 203-236. doi:10.1016/j.ocemod.2004.02.001

Oke, P. R., P. Sakov, M. L. Cahill, J. R. Dunn, R. Fiedler, D. A. Griffin, J. V. Mansbridge, K. R. Ridgway, A. Schiller, 2013a: Towards a dynamically balanced eddy-resolving ocean reanalysis: BRAN3, *Ocean Modelling*, 67, 52-70,10.1016/j.ocemod.2013.03.008.

Oke, P. R., D. A. Griffin, A. Schiller, R. J. Matear, R. Fiedler, J. V. Mansbridge, A. Lenton, M. Cahill, M. A. Chamberlain, K. Ridgway, 2013b: Evaluation of a near-global eddy-resolving ocean model, *Geoscientific Model Development*, **6**, 591-615, doi:10.5194/gmd-6-591-2013.

Polton, J.A.; Lewis, D.M.; Belcher, S.E. (2005), The role of wave-induced Coriolis–Stokes forcing on the wind-driven mixed layer, Journal of Physical Oceanography, 35 (4): 444–457, Bibcode:2005JPO....35..444P, doi:10.1175/JPO2701.1

Qiao, F., Y. Yuan, T. Ezer, C. Xia, Y. Yang, X. Lu and Z. Song (2010) A three-dimensional surface wave-ocean circulation coupled model and its initial testing. *Ocean Dynamics,* 60, 1339-1355. Doi:10.1007/s10236-010-0326-y

Röhrs, J., Christensen, K.H., Hole, L.R. et al. Ocean Dynamics (2012) 62: 1519. do:10.1007/s10236-012-0576-y

Uchiyama, Yusuke, James C. McWilliams, Alexander F. Shchepetkin, 2010. Wave-current interaction in an oceanic circulation model with a vortex-force formalism: Application to the surf zone. Ocean Modelling 34, 16-35.

Warner JC, Armstrong B, He R, Zambon JB (2010) Development of a coupled ocean–atmosphere–wave–sediment transport (COAWST) modeling system. Ocean Model 35:230–244. doi:10.1016/j.ocemod.2010.07.010

8. APPENDIX 1: DATA MANAGEMENT

8.1 Raw dataset created

None

8.2 Data processing and derived datasets

Derived datasets were created by the model, as described herein.

8.3 Data curation and archive

Model output will be curated by SARDI and CSIRO but is not expected to be of lasting value, since improvements to the model renders old output obsolete.

8.4 Data access, use agreements and licensing

Model output is available on request.

8.5 Publication of datasets

Not anticipated.

9. APPENDIX 2: STUDENT PROJECTS

9.1 Student name

None

9.2 Degree type, project title and institution

9.3 Status of student project

10. APPENDIX 3: PROJECT PUBLICATIONS

10.1 Papers

None.

10.2 Presentations

Griffin D (2015). Surface waves: effects on circulation. Great Australian Bight Research Program Science Symposium, SARDI Aquatic Sciences, Adelaide, 19 August 2015.

Griffin D, Hertzfeld M, Hammer M and Oke P (2017). Circulation of the Great Australian Bight: the influence of waves and the Leeuwin Current. Australian Marine Sciences Association (AMSA) Conference 2017, Darwin, 2-6 July 2017.

Griffin D, Hertzfeld M, Hammer M and Oke P (2017). Circulation of the Great Australian Bight: the influence of waves and the Leeuwin Current. Great Australian Bight Research Program Science Symposium, SARDI Aquatic Sciences, Adelaide, 9th August 2017.

10.3 Patents

None

10.4 Media Releases

None

11. APPENDIX 4: INTELLECTUAL PROPERTY

11.1 Unique discoveries

None

11.2 Action plan

Future related work at SARDI and CSIRO will build on the work reported here and will acknowledge the Great Australian Bight Research Program.

12. APPENDIX 5: REVIEW OF WAVE-OCEAN COUPLING

The development of hydrodynamic models to include wind-wave dependent processes within the model physics has been a priority for several research groups in recent years. Here we provide an overview of coupled wave-hydrodynamic models which have been developed, including an outline of the processes which have been considered within each model.

The ECMWF have recently undertaken developments of their coupled atmosphere-wave-ocean model, to investigate surface wave effects in the ocean component of the model (Breivik et al., 2015). They extended the model to investigate three physical processes related to ocean surface waves (surface stress, modified by growth and dissipation of the oceanic wave-field), the turbulent kinetic energy flux from breaking waves, and the Stokes-Coriolis force. The effects of these processes were investigated in both forced 'wave-ocean' experiments (most relevant to our study), as well as in the fully-coupled atmosphere-wave-ocean system. All three processes were noticeable, particularly in the extra-tropics, but the sea-state-dependent turbulent kinetic energy flux had the greatest effect.

The US Naval Research Laboratory Coupled Ocean/Atmosphere Mesoscale Prediction System (COAMPS) model has recently undergone development to include wave coupled processes (Allard et al., 2014). The system is a fully coupled atmosphere-wave-ocean model system, and incorporated

surface stress processes applied similarly to that as outlined above for the ECMWF model. The model uses ocean currents as input to the wave model, to improve simulation of the wave field, and includes wave model output to investigate the effects of the Stokes-Coriolis force. The Stokes Drift is also used in the parameterisation of the enhancement of vertical mixing by Langmuir turbulence (LT), as described by Kantha and Clayson (2004), and added to the TKE and vertical turbulent length-scale equations in a Mellor-Yamada 2.5 turbulence model. It is worth noting that Harcourt (2012) argues the Kantha-Clayson parameterisation underestimates the additional shear-production terms as it overlooks the momentum flux of turbulence down-Stokes gradient. While the LT is parameterised, it is acknowledged that LT generation under hurricane conditions will be minimal owing to the misalignment between wind and waves under these conditions.

The USGS Coupled Ocean-Atmosphere-Wave-Sediment Transport (COAWST) Modelling System (Warner et al., 2010) includes a range of sea-state-dependent processes. These include wave-dependent parameterisations of drag in the atmospheric model (somewhat consistent with ECMWF). In the ocean model, the wave fields are used to compute 1) forcings in the form of radiation stress gradients (2-D) that create wave-driven flows in shallow water, 2) Stokes velocities for estimating the Stokes-Coriolis and other terms in the momentum equation, and 3) wave-enhanced bottom stresses. The wave model receives varying water levels and ocean currents from the ocean model, and morphological changes from the sediment transport model.

Roland et al (2012) developed a fully coupled 3D wave-current model. Three sea-state dependent processes were parameterised into the ocean model, including (1) the wave momentum flux that can be represented by 'radiation stresses' (Longuet-Higgins and Stewart, 1962); (2) surface mixing following Craig and Banner, 1994); (3) wave-induced bottom stress in shallow waters (Grant and Madsen, 1979). The effects of currents on the wave field (current-induced Doppler shift) were parameterised into the wave model.

Qiao et al (2004) (and consequent papers) have investigated the influences of wave-induced mixing of the upper ocean in a global ocean circulation model. They proposed a parameterisation of mixing owing to the high Reynolds numbers of the orbital motion of non-breaking waves (the Bv scheme), which appears similar to the mixing explored by Babanin (2006), Babanin and Haus (2009) and Ghantous and Babanin (2013). The wave-induced vertical viscosity Bv is defined and used as a parameter to estimate the strength of wave mixing, and is added to the vertical diffusivity in a global ocean circulation model. They suggest that this improved the temperature structure of the upper 100m relative to the observed climatology.

Fan and Griffies (2014) investigated the effects of parameterised upper-ocean mixing on global climate simulations, through modification of the Large et al. (19XX) K-profile ocean boundary layer parameterisations in a coupled atmosphere-ocean-wave global climate model. Three parameterisations were considered: (1) The McWilliams and Sullivan (2000) parameterisation of Langmuir turbulence enhancement to the nonlocal component of KPP; (2) the Smyth et al (2002) parameterisation which modifies the McWilliams and Sullivan scheme by adding a stratification effect to restrain the turbulent enhancement under weak stratification conditions (e.g., winter) and enhance under strong stratification conditions; and (3) the Qiao et al (2004) parameterisation of mixing by non-breaking waves, which adds a wave orbital velocity to the Reynolds Stress calculation. Analysis focused on the effects to high-latitude ocean mixed layer depths and related ocean diagnostics. Scheme 1 lead to too large an influence in winter, with overly deep mixed layers created, and minimal impact in summer. Scheme 3 provided the strongest summer mixed layer deepening in the Southern Ocean, with weak impacts in winter. Scheme 2 improved winter mixed

layer depth simulations with mixed layer deepening in polar seas and was identified as a key element for improving mixed layer simulations.

At NOC, the coupled POLCOMS-WAM system was described by Brown et al. 2011. The POLCOMS model has been developed to include a Mellor-Yamada turbulence closure modified to consider surface wave breaking (Craig and Banner, 1994). The wave model is driven by currents and sea-level from the POLCOMS model, to account for the Doppler shift of the waves, and the Madsen (1994) wave-current bottom friction. The hydrodynamic model is developed to include wave-enhanced bed friction and a wave-enhanced surface friction, in addition to the Stokes-Coriolis term, and 3D radiation stress terms as defined by Mellor (2003). The Mellor (2008) terms were also coded and tested, but found to be unstable in the offshore zone (depths 30-50m). The Mellor (2003) method was considered applicable for areas of low bottom gradients, as found in their study region in Liverpool Bay. The inclusion of this scheme was found to have high computational overhead. For deep microtidal regions, it was suggested that the Stokes drift has the dominant effect on the current field, and the radiation stress is of little importance. Conversely, in a shallow macrotidal regime, it was suggested that the radiation stress terms are larger, and the Stokes drift has minimal effect.

The HZG group have developed a coupled wave-ocean model to support their coastal-ocean prediction systems (Staneva et al., 2014). The WAve Model WAM has been coupled with the General Estuarine Transport Model (GETM) hydrodynamic model, taking into consideration the effect of currents on waves, and the effects of waves on upper ocean dynamics – in particular on mixing and drift currents. GETM was modified to account for wave effects by introducing a wave-enhanced bottom friction, including turbulent kinetic energy flux due to wave breaking, following the theme of Craig and Banner (1994), and the Stokes-Coriolis force. This model also introduces 3D depth-dependent (3D) radiation stresses. Reflecting the scientific dispute regarding process, they have parameterised both the Mellor (2011) radiation stress formulation, and the Vortex Force formulation proposed by Ardhuin et al, (2008) and Bennis et al., 2011, as alternative parameterisations. Moghimi et al. (2013) compared the effects of these two parameterisations, and concluded the Mellor model introduced shortcomings in the model in wave-shoaling regions situated at steep slopes, suggesting this method should be limited to applications with short period waves and mild bottom slopes. The Vortex Force approach also had shortcomings, but was proposed as a more prospective model for research in the field. In the initial stage of development, adopting the radiation stress formulation originally proposed by Longuet-Higgins and Stewart (1962, 1964) seems appropriate.

Synthesising the above review of just some of the coupled hydrodynamic-wave models which have been developed in recent years, we observe that there are broadly two categories of interest. One is focused towards shelf and coastal studies, interested in the effects of wave-driven currents (and possibly effects of bottom friction), and the second are the broad scale (global) ocean models interested in improving parameterisations of mixing to ensure that surface ocean mixed layers are well represented, to aid simulation of the large scale ocean processes.

The Great Australian Bight region spans the features of interests of these two communities. We have placed little priority on parameterising the radiation stress terms, owing to their expected minor influence in the area of the BP mooring, and have thus focused efforts on parameterising and assessing the effects of the Stokes-Coriolis forcing and effects of wave-enhanced vertical mixing.

References

Allard, R., E. Rogers, P. Martin, T. Jensen, P. Chu, T. Campbell, J. Dykes, T. Smith, J. Choi, and U. Gravois. 2014. The US Navy coupled ocean-wave prediction system. *Oceanography* 27(3):92–103, http://dx.doi.org/10.5670/oceanog.2014.71.

Ardhuin, F., Rascle, N., Belibassakis, K. (2008). Explicit wave-averaged primitive equations using a generalized Lagrangian mean. Ocean Modell., Vol. 20 (1), 35 60.

Babanin, A. V., 2006. On a wave-induced turbulence and a wave-mixed upper ocean layer, Geophys. Res. Lett., 33, L20605, doi:10.1029/2006GL027308.

Babanin, A. V. and Haus, B. K., 2009. On the existence of water turbulence induced by nonbreaking surface waves, J. Phys. Oceanogr., 39, 2675–2679.

Bennis, A., Ardhuin, F. (2011). Comments on the depth-dependent current and wave interaction equations: a revision. J. Phys. Oceanogr., Vol. 41, 2008 2012.

Breivik, O., K. Mogensen, J-R Bidlot, M.A. Balmaseda, PAEM Janssen, 2015. Surface wave effects in the NEMO ocean model: Forced and coupled experiments. J. Geophys. Res: Oceans.

Brown, J.M., Rodolfo Bolaños, and Judith Wolf (2011) Impact assessment of advanced coupling features in a tide–surge–wave model, POLCOMS-WAM, in a shallow water application, Journal of Marine Systems, Volume 87, Issue 1, July 2011, Pages 13-24, doi:10.1016/j.jmarsys.2011.02.006.

Craig, P. D., and M. L. Banner (1994), Modeling wave-enhanced turbulence in the ocean surface layer, *J. Phys. Oceanogr.*, **24**(12),2546–2559, doi:10.1175/1520-0485(1994)024<2546:MWETIT>2.0.CO;2.

Fan, Y. and Stephen M. Griffies, 2014: Impacts of Parameterized Langmuir Turbulence and Nonbreaking Wave Mixing in Global Climate Simulations. *J. Climate*, **27**, 4752–4775. doi: http://dx.doi.org/10.1175/JCLI-D-13-00583.1

Ghantous, M. and Babanin, A. V.: One-dimensional modelling of upper ocean mixing by turbulence due to wave orbital motion, Nonlin. Processes Geophys., 21, 325-338, doi:10.5194/npg-21-325-2014, 2014.

Grant, W. D., and O. S. Madsen (1979), Combined wave and current interaction with a rough bottom, *J. Geophys. Res.*,**84**(C4), 1797–1808, doi:10.1029/JC084iC04p01797.

Harcourt, R.R. 2013: A Second-Moment Closure Model of Langmuir Turbulence. *J. Phys. Oceanogr.*, **43**, 673–697. doi: http://dx.doi.org/10.1175/JPO-D-12-0105.1

Jones, N.L. and S.G. Monismith, "Modeling the influence of wave enhanced turbulence in a shallow tide-and wind-driven water column," J. Geophys. Res., 113, C03009, doi: 10.1029/2007JC004246 (March 2008)

Kantha, L.H., and C.A. Clayson. 2004. On the effect of surface gravity waves on mixing in the oceanic mixed layer. *Ocean Modelling* 6:101–124, http://dx.doi.org/10.1016/S1463-5003(02)00062-8.

Longuet-Higgins, M. S., and R. W. Stewart (1962),Radiation stress and mass transport in gravity waves, with application to 'surf beats', *J. Fluid Mech.*,**13**(04), 481–504, doi:10.1017/S0022112062000877.

Longuet-Higgins, M. S., R. W. Stewart, Radiation stresses in water waves; a physical discussion, with applications, *Deep-Sea Res.*, **11**, 529–562, 1964.

McWilliams, J. C., and P. P. Sullivan, 2000: Vertical mixing by Langmuir circulations. *Spill Sci. Technol. Bull.*, **6**, 225–237, doi:10.1016/S1353-2561(01)00041-X

Mellor, G. 2003. The three-dimensional current and surface wave equations**,** Journal of Physical Oceanography, 33 (9) (2003), pp. 1978–1989

Mellor, G. 2008. The depth-dependent current and wave interaction equations: a revision**,** Journal of Physical Oceanography, 38 (11) (2008), pp. 2587–2596

Mellor, G.L. (2011) Corrigendum. J. Phys. Oceanogr., 41, 1417 – 1418

Moghimi, S., Klingbeil K., Gräwe U., Burchard H. (2013). A direct comparison of a depth dependent Radiation stress formulation and a Vortex force formulation within a three dimensional coastal ocean model. Ocean Modelling, Vol. 70, 132-144

Qiao, F., Y. Yuan, Y. Yang, Q. Zheng, C. Xian and J. Ma (2004). "Wave-induced mixing in the upper ocean: Distribution and application to a global ocean circulation model", Geophysical Research Letters, Vol. 31, L11303, dio:10.1029/2004GL019824.

Roland, A., Y. J. Zhang, H. V. Wang, Y. Meng, Y.-C. Teng, V. Maderich, I. Brovchenko, M. Dutour-Sikiric, and U. Zanke (2012), A fully coupled 3D wave-current interaction model on unstructured grids, J. Geophys. Res., 117, C00J33, doi:10.1029/2012JC007952.

Staneva, J., and K. Wahle, 2014. Coupling of Wave and Circulation Models in Coastal-Ocean Predicting Systems: A case study for the German Bight. Proc. 17th Physics of Estuaries and Coastal Seas (PECS) conference, Brazil.

Smyth, W. D., E. D. Skyllingstad, G. B. Grawford, and H. Wijesekera, 2002: Nonlocal fluxes and Stokes drift effects in the *K*-profile parameterization. *Ocean Dyn.*, **52**, 104–115, doi:10.1007/s10236-002-0012-9.

Warner, J.C.**,** Armstrong, B., He, R., and Zambon, J. **(**2010). Development of a Coupled Ocean-Atmosphere-Wave-Sediment Transport (COAWST) Modeling System, Ocean Modelling, 35, 230-244. http://dx.doi.org/10.1016/j.ocemod.2010.


bp


CSIRO


SOUTH AUSTRALIA
Government
of South Australia
Primary Industries
and Regions SA


SARDI
SOUTH AUSTRALIAN
RESEARCH AND
DEVELOPMENT
INSTITUTE


SUB CRUCE LUMEN
THE UNIVERSITY
of ADELAIDE


Flinders
UNIVERSITY